ftn Associates Ltd.
water resources / environmental consultants

MID-BARATARIA SEDIMENT DIVERSION (BA-0153)

MODELING EFFECTS OF THE PROPOSED PLAQUEMINES LIQUIDS TERMINAL ON THE MID-BARATARIA SEDIMENT DIVERSION

PRELIMINARY

FOR REVIEW ONLY

Ranjit Jadhav, PhD, PE
LA No. 29984

COASTAL PROTECTION AND RESTORATION AUTHORITY
CPRA

DRAFT
FEBRUARY 18, 2020

AECOM

MID-BARATARIA SEDIMENT DIVERSION
(BA-0153)

MODELING EFFECTS OF THE PROPOSED PLAQUEMINES LIQUID TERMINAL ON THE MID-BARATARIA SEDIMENT DIVERSION

Prepared for

AECOM Technical Services
7389 Florida Blvd.
Suite 300
Baton Rouge, LA 70806

Prepared by

FTN Associates, Ltd.
7648 Picardy Avenue, Suite 100
Baton Rouge, LA 70808

FTN No. R05540-1566-006

DRAFT
February 18, 2020

TABLE OF CONTENTS

TABLE OF CONTENTS (CONTINUED)

LIST OF TABLES

LIST OF FIGURES

LIST OF FIGURES (CONTINUED)

LIST OF FIGURES (CONTINUED)

LIST OF FIGURES (CONTINUED)

1.0 INTRODUCTION

This report describes the hydraulic, sediment transport and morphological analysis performed using numerical models to evaluate the effect of the proposed Plaquemines Liquids Terminal (PLT) project on the performance of the Mid-Barataria Sediment Diversion (MBSD) project. FTN Associates, Ltd. (FTN) performed the study as a member of the Design Team (DT) led by the AECOM Technical Services (AECOM). The DT is providing the Engineering and Design (E&D) services for the MBSD project to the Coastal Protection and Restoration Authority (CPRA) of Louisiana. The DT is currently performing the 30% Level E&D analysis. Royal HaskoningDHV Consultants (RHDHV) provided the Independent Technical Review (ITR) of this study.

The proposed PLT facility is situated about 1,500 ft upstream of the MBSD intake on the west bank of the Mississippi River (MR) and 2500 ft downstream of the existing Cenex Harvest States Inc. (CHS) grain terminal.

2.0 PURPOSE, SCOPE AND LIMITATIONS

The purpose of the modeling study is to add the proposed PLT facility to the numerical models developed for the MBSD and evaluate the effects on the water level, velocity, discharge and sediment transport in the MR and in the diversion canal.

The modeling study is limited to the MR segment in the vicinity of the diversion structure, i.e., about 5 miles upstream and downstream of the diversion intake which is the approximate extent of the primary model domains. The effect of the Mid-Breton diversion proposed at approximately RM 68 on the east bank of the MR is not considered in this study.

The models are not setup to provide information for the design of the structural components of the PLT facility. The MBSD E&D is currently at the 30% level and the numerical model geometry incorporate diversion components designed at this level. Further E&D efforts are underway, and the models and results are subject to change.

3.0 METHODOLOGY

The modeling method is described in the flow-chart shown on Figure 3.1. A combination of two-dimensional (2D) and three-dimensional (3D) Delft3D models along with the 3D FLOW-3D Computational Fluid Dynamic (CFD) model is used to simulate the effects of PLT on the MBSD as shown in the Figure 3.1.

3.1 General Approach

The 3D FLOW-3D model included a segment of the MR with- and without-PLT, the intake headworks and a portion of the conveyance channel (CC). This model was primarily used to simulate the non-hydrostatic flow field (water level and velocity) and energy losses in the system through steady-state (SS) runs.

The 3D Delft3D (hydrostatic) model covered the similar model extent and was calibrated using SS runs to the energy losses provided by the FLOW-3D model. This model was primarily used to simulate the MR morphology, sediment transport and the discharge and sediment load through the diversion. The production runs were performed using one-year MR hydrograph.

The 2D Delft3D model (hydrostatic) covered the above model domain with the addition of the entire diversion channel and the Barataria Basin up to the Gulf of Mexico. It was calibrated using SS to the energy losses provided by the FLOW-3D model. The purpose of this model was to provide realistic water level (WL) boundaries to the partial conveyance channel (CC) segment represented in the 3D models. Performing 3D model simulations with the entire conveyance channel and the Barataria Basin would have been prohibitively costly and time consuming without any added accuracy to the study.

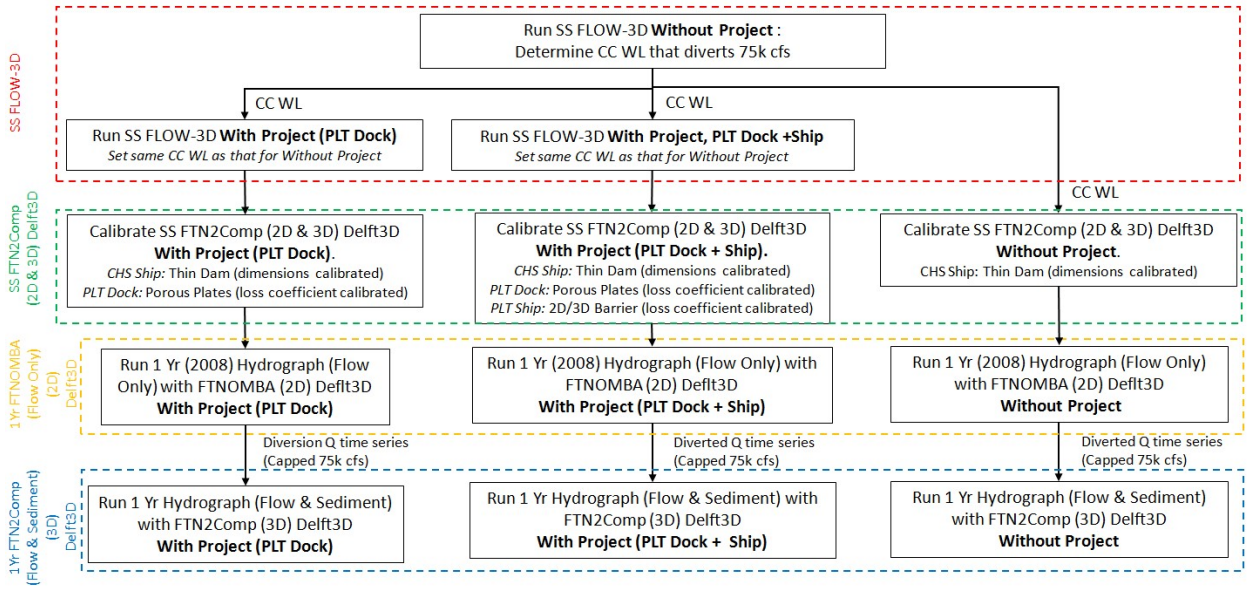

Figure 3.1. Flow-chart showing sequence, purpose, and setup of the various models used in this study.

3.2 Modeling Programs

Considering the important hydraulic processes and the previous work by the Water Institute of the Gulf (WI) and CPRA, two multi-dimensional modeling programs were selected, namely, FLOW-3D and Delft3D. The modeling programs are briefly described below in the following sections.

3.3 FLOW-3D Modeling

Several CFD models exist that can be used to model the MBSD diversion. In this application, it is imperative that the model has the ability to efficiently solve for the spatial and temporal variations in water levels as well as the turbulent three-dimensional near-field flow velocities produced as a result of fluid structure interaction at the intake. The FLOW-3D three-dimensional (3D) CFD software licensed from Flow Science, USA (Flow Science, 2018) was selected as the appropriate modeling tool for the near-field hydrodynamic and the suspended sediment transport modeling. FLOW-3D was used previously by CPRA/WI to model the flow and suspended sediment through sediment diversions during the planning phase (Meselhe et al., 2012). It was proven to be able to capture the complex 3D flow field in the vicinity of the

diversion as well as quantify the spatial distribution of the suspended sediment on the lateral bar near the diversion. FLOW-3D was also used in the study by HDR Engineering as described in the 30% design report (HDR, 2014) for screening of diversion alternatives. FLOW-3D is currently the only available commercial CFD model capable of simulating suspended sediment in free surface flows over complicated river bathymetries, irregular banks and intake structure using structured grids (Allison et al., 2017). Since FLOW-3D solves the complete 3D Reynolds-Averaged Navier-Stokes equations with turbulence closure, it is inherently non-hydrostatic and gives more accurate vertical flow profiles than models that are based on the shallow water equations. However, the model is computationally intensive, with relatively long computational times for this application. Therefore, the FLOW-3D analysis was only applied to selected steady-state flow conditions, which are representative snapshots from a typical river hydrograph. The model was used to determine the energy loss through the system and the Sediment-Water Ratio (SWR, described later) using a discrete particle tracking model. One limitation of FLOW-3D is that, at this time, it does not include a validated and efficient model for simulating sediment transport together with morphology change (i.e., the bed level change due to erosion and deposition of sediment) near the diversion. Therefore, the morphology change analysis was performed using another modeling software called Delft3D described later in this report.

3.3.1 Model Geometry

A FLOW-3D model named FTNMSDI was developed to model the hydrodynamic effects of the PLT dock structure and the ship on the MBSD diversion intake. The FLOW-3D model geometry extended in the MR from River Mile (RM) 58.1 downstream to RM 65 upstream (All river miles referenced are relative to the Head of Passes which is at RM 0). The details of the domain extent and the mesh blocks are shown on Figure 3.2.

The FTNMSDI model is being used currently for E&D of the MBSD project. One of the key improvements made to the FTNMSDI model developed here over the previous FTNMSDI model, was that the upstream boundary in the current FTNMSDI model has been extended further north upstream to RM 65.0 from the RM 62.7 location in the previous FTNMSDI model.

This was done after initial model runs with the PLT Dock showed that the previous boundary location in the FTNMSDI model was too close to the PLT location and showed upstream boundary effects on the calibration results at the transect crossing near the proposed PLT location. Moving the boundary approximately 2 miles upstream in the updated FTNMSDI model resolved this issue. Note that the choice of the FTNMSDI boundary at RM 62.7 is still appropriate for the MBSD modeling results (without the PLT) because the upstream boundary effects are negligible at the MBSD intake for either choice of the upstream locations, i.e., the flow from the upstream is already developed when it reaches the MBSD location. The upstream boundary extension is only required in the current FTNMSDI model since the study site of interest (PLT Dock and Ship) which is approximately 1500 ft upstream of the MBSD location is also affected by the CHS terminal which is about a mile upstream of MBSD, an extension of the upstream boundary captures the combined effect of all these features in the model. A second change made to the model was the inclusion of the CHS terminal into the updated FLOW-3D FTNMSDI model which is approximately 0.5 mile upstream of the PLT location and whose effect cannot be neglected when modeling hydrodynamic effects at PLT.

The bathymetry for the river portion of the model was generated by combining multibeam survey data from US Army Corps of Engineers (USACE). The 2012 USACE channel survey (published in 2013) was used for the main channel and the 2017 USACE revetment surveys were used for the revetment portions in the river. The bathymetry for the MBSD intake and conveyance channel used the latest design by the DT for CPRA.

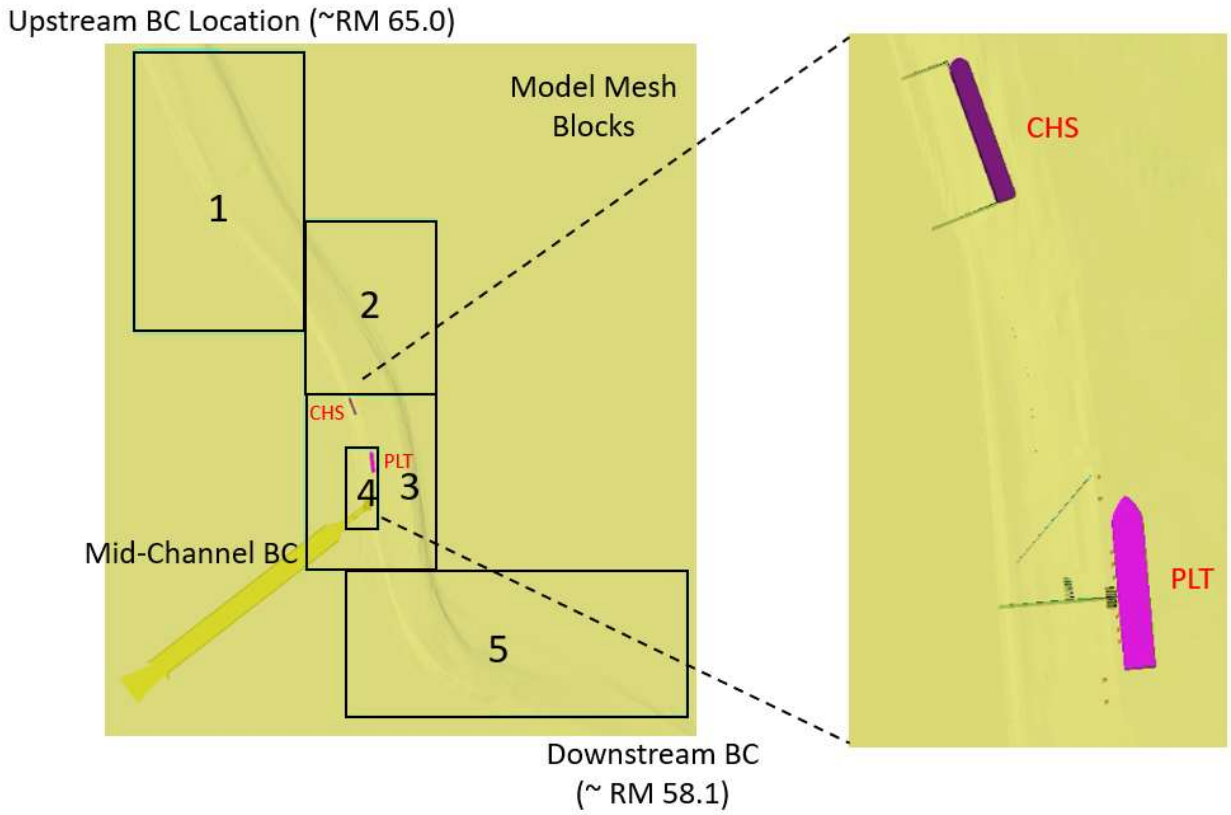

Figure 3.2. Model domains, mesh blocks and boundary locations of the FTNMSDI FLOW-3D model and their relation to the CHS and PLT terminals.

3.3.2 PLT model setup

The structural drawings for the proposed PLT Dock structure and ship, while docked at the PLT Dock, were provided by Tallgrass Energy. All underwater structures with possible hydrodynamic impacts (e.g., the ship, the barge deflector, the access-way, the fire-water intake platform, the liquid loading platform, and the breasting and mooring dolphins) were identified for distinct representation in the model. The PLT ship is modeled as a solid body. The ship is assumed to be loaded up to approximately half its full draft (modeled as having a mean draft of 28 ft), and is assumed to be present for the entire operational period of the diversion for the one year hydrograph period simulated.

Figure 3.3 and Table 3.1 show the details of the PLT structures and the ship as represented in the FLOW-3D model. The individual piles and dolphins are too small to be

resolved at the individual fluid-structure interaction scale, using the river reach-scale model grid. Instead they were represented by sub-grid scale drag effects of the structures by mesh planes, which can be appropriately parameterized to extract energy from the main flow, without the need to resolve the individual wake of each pile structure in detail. This approach has been used before in Meselhe et al. (2012) and is also used here to model drag effects of the pile arrays (access-way, barge deflector, fire-water and liquid loading platforms), truss and individual dolphins (which are too small to be resolved independently but still have non-negligible drag effects on the global flow) by porous mesh planes. The group of barges with a uniform 3 ft draft arranged continuously on top of the barge deflector pile group is represented by a solid mesh plane (negligible width). The ship at the PLT Dock can be fully resolved at the model grid scale and is modeled as a solid body. Explanations of the choice of model coefficients for the porosity, linear loss coefficient and the quadratic loss coefficient for the mesh planes are provided in the following paragraphs. These coefficients were carefully chosen to parameterize complex drag effects of the major structural configurations based on the theoretical and empirical studies found in the literature.

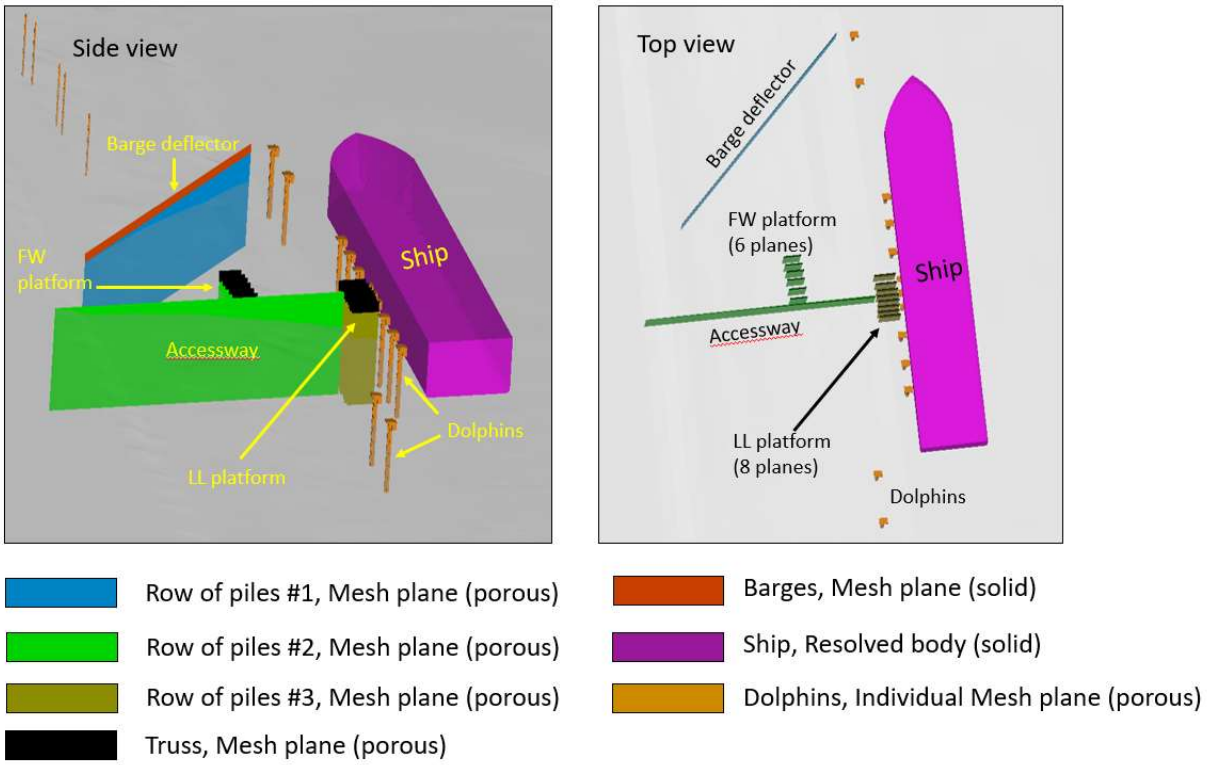

Figure 3.3. Illustration of the PLT structures in the FTNMSDI FLOW-3D model.

Table 3.1. Modeling details of the PLT components in FLOW-3D.

PLT structures	Mesh plane type	Vertical extent	Porosity (ε)	Linear loss coefficient (KBAF1)	Quadratic loss coefficient (KBAF2)
Accessway and Firewater platforms: row of piles	Mesh plane (porous)	Extends from river bed up to 3 ft, NAVD88	0.90	0.16	0.00
Liquid loading platforms: row of piles	Mesh plane (porous)	Extends from river bed up to 3 ft, NAVD88	0.86	0.16	0.00
Fire-Water and Liquid-Loading platforms: truss	Mesh plane (porous)	Extends from 3 ft, NAVD88 up to 14.5 ft, NAVD88	0.78	0.00	0.90
Barge deflector: row of piles	Mesh plane (porous)	Extends from river bed up to 3 ft below water surface	0.96	0.16	0.00
Barge deflector; barges	Mesh plane (solid)	Extends from 3 ft below water surface up to 12.4 ft, NAVD88	0.00	N/A	N/A
Dolphins	Individual Mesh plane (porous)	Extends from river bed up to 12.4 ft, NAVD88	1.00	0.00	1.00
Ship	No Mesh Plane, Resolved body (solid)	Extends from 28 ft (mean draft) below water surface up to 14.5 ft, NAVD88	N/A	N/A	N/A

The drag induced by a mesh plane on the main flow is represented by a pressure drop term in the Reynolds-Averaged Navier-Stokes (RANS) equations for incompressible flow. The pressure drop in FLOW-3D is calculated using a Darcy-Forcheimmer type equation (FlowScience 2018) as given below:

$$\Delta p = \rho \cdot (KBAF1 \cdot u + KBAF2 \cdot u|u|) \quad (1)$$

Where, Δp is the pressure drop in the flow direction per unit length, kg/m^2/s^2;
ρ is the density of water, kg/m^3;
u is the subgrid scale (within pile array) velocity, m/s with the following equation.

$$u = \frac{U_{bulk}}{\varepsilon} \quad (2)$$

Where, U_{bulk} is the velocity at the resolved scale of the bulk flow, m/s;

ε is the porosity which a measure of the void space in the structure. $KBAF1$ is the linear loss coefficient, 1/s, with the following equation:

$$KBAF1 = \frac{\upsilon}{k} \qquad (3)$$

Where, n is the kinematic Viscosity of water, m^2/s; k is the permeability, m^2;
KBAF2 is the quadratic loss coefficient, 1/m;
For approximation of the pressure drop across a row of piles, Chamsri et al., 2015 proposed the following equation

$$k = \frac{2\pi\varepsilon^{\ 2}}{(1-\varepsilon)R_e C_d} \quad (4)$$

Where, ε is the porosity; r is the diameter of the pile, m; $R_e = uD/\nu$ is the Reynold's number based on individual pile diameter (D); C_d is the drag coefficient for the individual pile.

Table 3.2. Reynolds number for different cylindrical piles used in PLT Dock components. (DAV is Depth-Averaged Velocity).

Structure	Pile Diameter (D) (ft)	Porosity	MR Flow (cfs)	Estimated MR DAV at PLT (ft/s)	Estimated Local DAV in Pile Array (ft/s)	Pile Reynolds Number (Re)
Accessway Piles	1.5	0.90	1,000,000 (High Flow)	4.0	4.4	6.2 E5
			600,000 (Low Flow)	2.0	2.2	3.1 E5
Barge Deflector Piles	4.0	0.96	1,000,000 (High Flow)	4.0	4.2	1.5 E6
			600,000 (Low Flow)	2.0	2.1	7.7 E5
Breasting Dolphins	9.0	1.00	1,000,000 (High Flow)	4.0	4.0	3.3 E6
			600,000 (Low Flow)	2.0	2.0	1.7 E6

Achenbach's (1971) pile drag coefficient variation (Figure 3.4) versus the pile Reynolds number chart was used to determine the C_d for an individual pile. The Reynolds number computations at high and how flows for the various cylindrical members are shown in Table 3.2. Equations 2 through4 were used to derive the values for the linear loss coefficient for the different pile arrays. As an example of how the linear loss coefficient for the accessway piles is calculated, consider the accessway pile array which has piles with diameter of 1.5 ft spaced apart 15 ft across the streamwise direction. The porosity (ε) for the accessway pile structure in the streamwise direction thus is 0.9 (=1-1.5/15). For MR flow ranging from 600,000 cfs to 1,000,000 cfs, the depth-averaged velocity (DAV) in the bulk flow (U_{bulk}) around the PLT dock structure varies approximately between 2 to 4 ft/s. With the porosity of 0.9, the local sub-grid scale DAV around the piles (u) can vary from 2.2 to 4.4 ft/s as given by Equation 2 above. This yields a pile Reynolds number range from 3.1 x 10^5 to 6.2 x 10^5 (Table 3.2). Figure 3.4 highlights this range and assuming a pile roughness (ks/D), where k_s is the Nikuradse's roughness length and D the pile diameter, of 1 to 5 x 10^{-3} for typical rough piles, the drag

coefficient of a single cylindrical pile, C_d can be estimated to be between 0.9 to 1.2. Applying equation (4), the permeability k, is calculated to be between 4.8 to 9.6 x10^{-6} m^2. The KBAF1 from equation (3) thus varies between 0.1 /m to 0.22 /m. For simplification, a mean of 0.16 /m was used in the model. As is shown in Table 3.1, the structure of rows of piles in the accessway, fire-water platform, liquid-loading platform and barge deflector was thus approximated with a linear loss coefficient of 0.16/m.

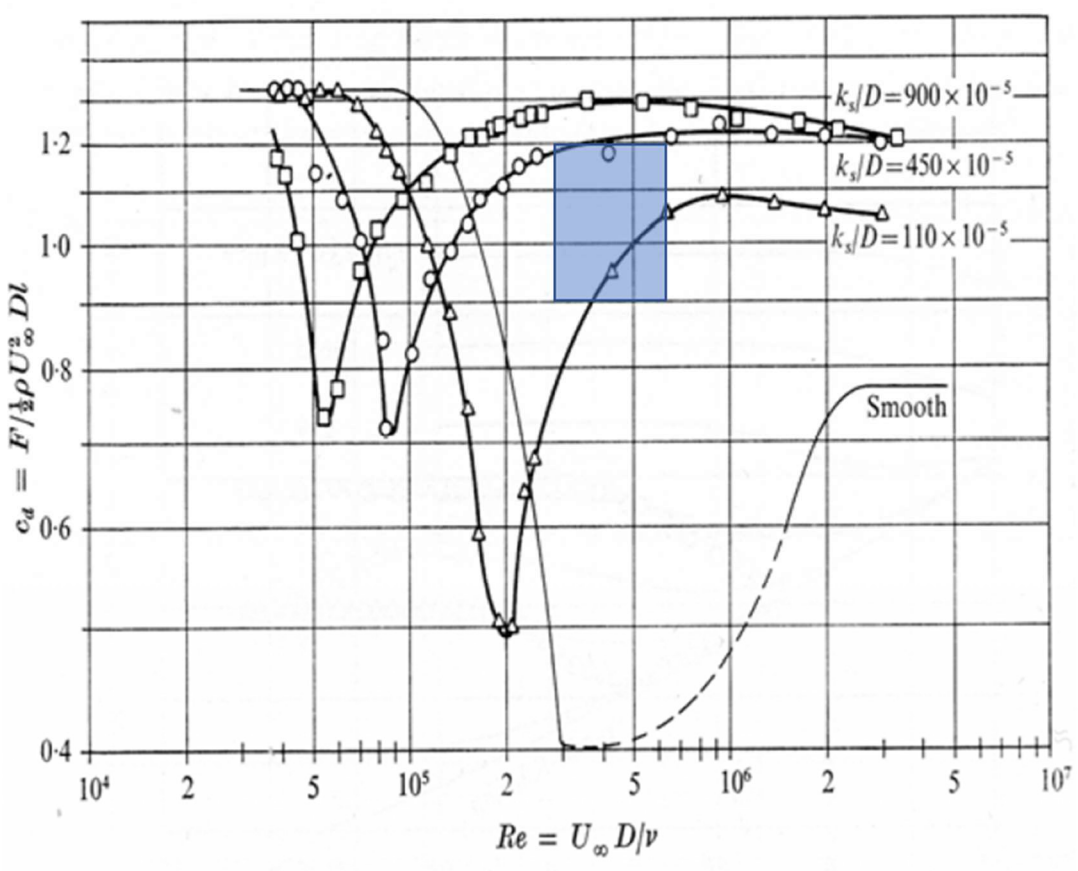

Figure 3.4. Individual cylindrical pile drag (C_d) variation with pile Reynolds number (Achenbach 1971).

The truss structures for the liquid-loading platform and fire-water platform are approximated with a quadratic loss coefficient (Blevins, 1984). This approach is similar to the method of representing truss drag effects by the quadratic drag law that was used by the WI (Meselhe et al., 2012). Figure 3.5 shows the table from Blevins (1984) which provides values for

empirical quadratic drag coefficients for open frame at different solidarity ratio (1-ε) and Reynold's number. With a solidarity ratio of 0.22 and Reynolds number greater than 5 x 10^5, the quadratic drag coefficient is determined to be 0.9 and is chosen for the mesh planes representing the firewater and liquid loading platform trusses for this study.

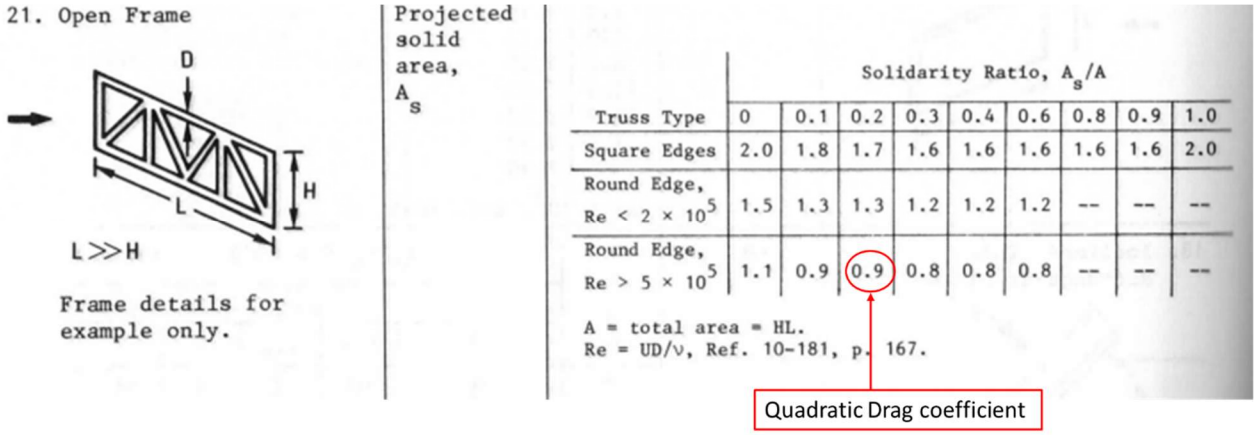

Figure 3.5. Quadratic drag coefficients for various solidarity ratios and Reynolds number range (Source: Table 10-19 from Blevins, 1984)

The barge section, which forms the top of the barge deflector, with a 3 ft draft below the water surface is considered impermeable by setting the porosity to 0 for that mesh plane; this leads FLOW-3D to disregard equations 1 to 3 and instead treat the mesh plane as a solid body that blocks the flow through it. The PLT ship is fully resolved as a solid body in the model with a no-slip boundary condition at the solid surface. The ship draft was held constant at 28 ft below the water surface over various river flows as the mean draft of the ship provided by Tallgrass Energy. Thus, the vertical position of the ship bottom was set at different elevations based on the different water surface elevation for the high and low flow runs. The water surface from the 'Without-Project' run was used as the guidance to set the ship bottom elevation for the 'With-Project' (PLT Dock+ Ship) runs.

In addition, a ship, anchored to the river bed and moored at the CHS terminal, was modeled by a fully resolved solid body. The dimensions of the CHS ship were obtained from the outline of an image of an actual ship moored at this location shown in a recent Google Earth

image (2018) from a recent period as the calibration period. This ship was included in all the runs (without PLT, PLT Dock and PLT Dock+Ship). The CHS Dock structure was represented by three mesh planes, two perpendicular to the flow and one along the flow, as seen on Figure 3.2.

Since the main goal of the study is to model the effects at the MBSD intake with- and without-PLT project conditions over the entire period of modeling (1 year), the development of an acceptable invariant background condition over that entire period (same 1 year) is important. The following factors are unknown within the period when the observed data were recorded:

- Whether a CHS ship was parked at the CHS terminal,
- The exact CHS ship draft,
- Presence or absence of additional barges along the right descending bank downstream of CHS, or
- The exact structural details of the CHS dock itself.

Therefore, it is reasonable to assume that once the model is calibrated/validated for a given setup, it can be considered as an acceptable background condition for the entire duration of the run. For the purposes of this study, this invariant background (Without-Project) condition, against which With-Project conditions can be evaluated for all the results presented, is considered to be the particular CHS setup against which the FTNMSDI model is calibrated against, i.e., which includes the effect of the CHS terminal and the anchored ship only.

3.3.3 Meshing and Boundary Conditions

Figure 3.6 show the extents of the mesh blocks and Table 3.3 shows the grid sizes within the five different mesh blocks. In order to better resolve the flow features near the PLT Dock, the FTNMSDI mesh that is used for the MBSD analysis was updated with enhanced local refinement (mesh block # 4) spanning from 150 ft upstream of PLT and to include the entire headwork of the MBSD diversion. Figure 3.6 shows both horizontal and vertical mesh grid sections near the PLT structure.

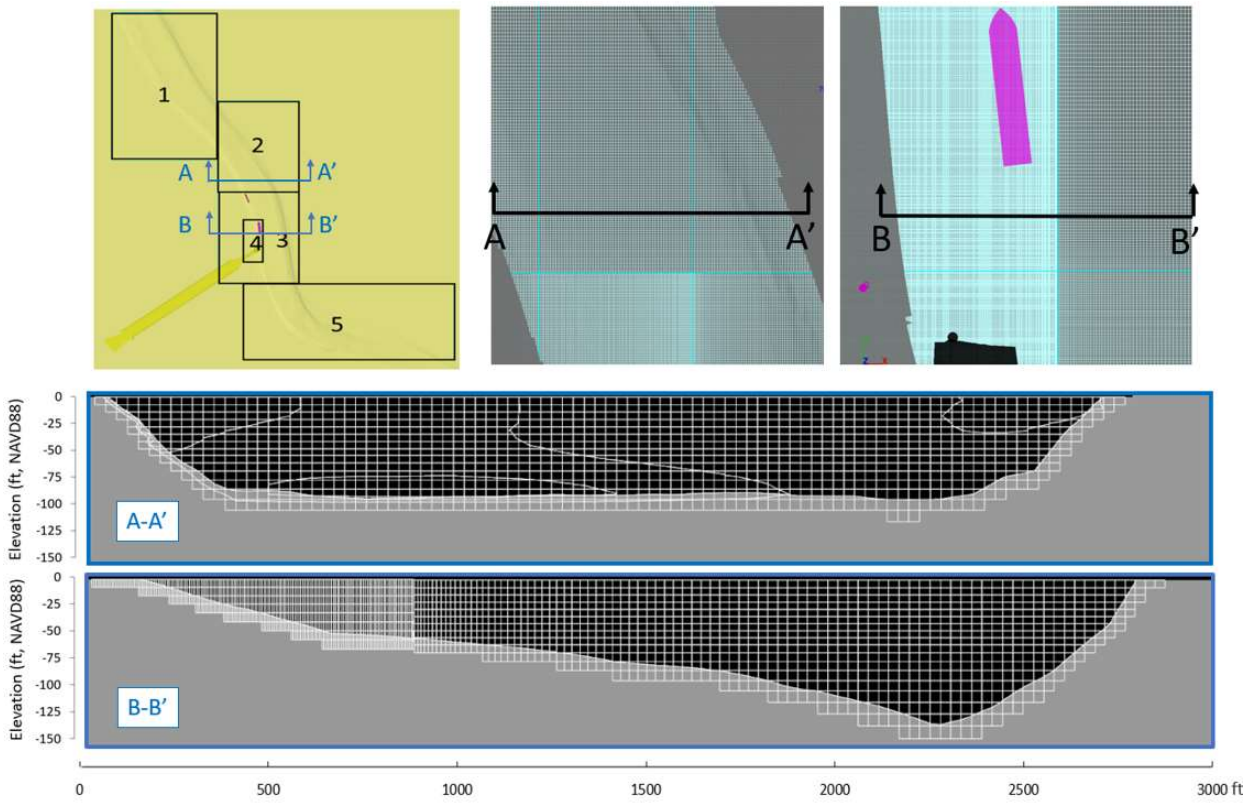

Figure 3.6. Illustration of the FLOW-3D horizontal mesh resolution and vertical resolution at two transects, A-A' and B-B'.

Table 3.3 Mesh sizes for the five mesh blocks in FLOW-3D.

Block No.	Δx (m)	Δy (m)	Δz (m)
1	10	10	1.8-3.5
2	8	5-10	1.8-3.5
3	2-8	3-8	1.8-3.5
4	1.3	1.3	1.8
5	5-8	5-8	1.8-3.5

A total of 11 run cases (2 runs for calibration/validation and 9 runs for production) were investigated as shown in Table 3.4. The MR upstream is specified by a discharge boundary condition as specified in Table 3.4. The MR downstream and mid-channel are set with a water level boundary condition. At MR flow at 1,000,000, 600,000 and 450,000 cfs, the corresponding water levels at downstream were set to 7.81 ft, 3.48 ft and 2.85 ft, based on stage-discharge (Q-H) relations determined from Delft3D runs under current (without MBSD) conditions. Note

that a slight drawdown in the water levels (approximately 1 ft maximum at high flows) in the river is expected due to the diversion operations. However, this cannot be determined apriori in the FLOW-3D model before ascertaining the diverted discharges through the diversion, which can only be determined from the Delft3D model including the basin effects, which in turn has to be first calibrated for PLT Dock and ship losses with FLOW-3D.

Hence, use of the existing condition (Without-Project) water levels in the FLOW-3D model may slightly overestimate the water level in the river compared to those determined from the Delft3D production runs that will be presented later in Section 5.3 and which includes the basin effects. The Delft3D production runs, particularly the sediment transport runs, use diverted discharge boundary condition at the mid-channel and thus include more accurate basin induced river drawdown effects.

For the purposes of FLOW-3D modeling it is appropriate to use boundary conditions without the slight (< 1 ft) drawdown effects in river water level due to the basin, as the main goal of the FLOW-3D runs is to develop data against which the Delft3D model can be calibrated later for losses at the PLT Dock and the ship. For the FLOW-3D model, the water levels at the channel-side boundary was set to 6.99 ft, 3.02 ft and 2.62 ft, respectively. These water levels, determined during the ongoing 30% E&D Level MBSD modeling study, allow the target diversion discharges (75,000, 48,000, 34,000 cfs respectively at 1,000,000 cfs, 600,000 cfs and 450,000 cfs MR flows) for the Without-Project cases.

For consistency, the same water levels were used for With-Project cases as well to study the hydrodynamic impact of the PLT structure. Therefore, the diverted discharge values from the FLOW-3D model, With- and Without-Project condition, are not true discharges as they neglect the basin effect and thus were not investigated. The role of the FLOW-3D model results is to simply provide hydrodynamic calibration data to the Delft3D models for PLT Dock and Ship induced energy loss effects on the MBSD.

Table 3.4. FLOW-3D model scenarios simulated.

Run #	MR discharge (cfs)	CHS Dock + Ship	Diversion Structure	PLT Dock	PLT Dock + Ship	Remark
1	1,060,000	Yes	No	No	No	Calibration, existing conditions
2	617,000	Yes	No	No	No	Validation, existing conditions
3	1,000,000	Yes	Yes	No	No	Diversion Open, existing conditions
4		Yes	Yes	Yes	No	Diversion Open, with PLT dock
5		Yes	Yes	Yes	Yes	Diversion Open, with PLT dock and ship
6	600,000	Yes	Yes	No	No	Diversion Open, existing conditions
7		Yes	Yes	Yes	No	Diversion Open, with PLT dock
8		Yes	Yes	Yes	Yes	Diversion Open, with PLT dock and ship
9	450,000	Yes	Yes	No	No	Diversion Open, existing conditions
10		Yes	Yes	Yes	No	Diversion Open, with PLT dock
11		Yes	Yes	Yes	Yes	Diversion Open, with PLT dock and ship

3.4 Delft3D Modeling

The Delft3D model (Deltares, 2018), solves the hydrostatic shallow water equations either in 2D or 3D mode (with sigma co-ordinates for the representation of vertical layers) and is suited for long term simulations over large spatial scales. The advantage of Delft3D is its ability to model morphology change with sediment transport (suspended and bedload) that is coupled with the hydrodynamics. Note that while FLOW-3D model is always used in 3D mode, the Delft3D model can be implemented both in 2D and 3D model. The Delft3D model was used extensively as the most reliable model for the long-term morphology and sediment transport modeling tasks by CPRA/WI during the planning phase (Meselhe et al., 2012a; Meselhe et al., 2015; Gaweesh et al., 2016; McCorquodale et al., 2016; Meselhe at al., 2017). It will remain as the model of choice for the MBSD project for long-term and large-scale simulation runs where the hydrostatic assumptions are valid. For the present modeling tasks, Delft3D will be used to

inform the hydraulic and sediment transport in the diversion channel, evaluate deposition/erosion in the MR, and develop flow rating curves.

3.4.1 Model Geometry and Boundary Conditions

Figure 3.7 shows the domains of the three models used in this study, along with the boundary conditions for each. The connection between the models and the hierarchy of their use is explained in the flowchart shown on Figure 3.1. The FTNMSDI FLOW-3D model presented in the previous section is shown in the right most panel for comparison. The two Delft3D models, the FTNOMBA (2D) and the FTN2Comp (3D) are shown in the left and middle panels.

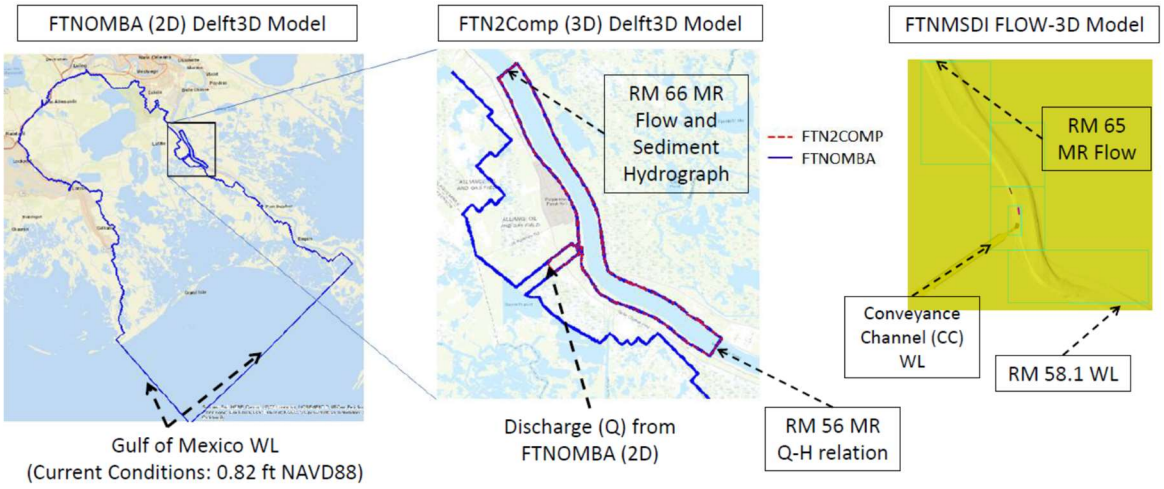

Figure 3.7. Model domains and boundary conditions: Delft3D model domains (left panel is the 2D FTNOMBA and mid-panel the 3D FTN2Comp), along with the FLOW-3D model domain (in right panel and as shown in Fig. 3.2 before).

Figure 3.8 shows the water discharge and sediment load hydrographs imposed at the upstream MR (RM 66) boundary for the 1-year production run. The 2008 hydrograph is selected as it is a good representative hydrograph of the last 15-year period (2004-2018). This hydrograph was also selected by Meselhe at al. (2017) to represent the period 2004-2013 in the WI Basin-wide model runs. The model data is post processed from the period when the MR discharge reaches 450,000 cfs (the trigger flow for diversion operation) in the rising limb up to the point when the MR discharge again falls just below 450,000 cfs in the falling limb. The

actual model run starts a few days earlier when the river is still below 450,000 cfs to allow enough time to overcome the initial conditions. The discharge at RM 66 is obtained from the Belle Chasse USGS gage daily historical data. The total sediment load is estimated from the Hysteresis Sediment Rating Curve (HSRC) developed by WI (Esposito et al., 2017) and the sand load from the Traditional Sand Rating Curve (TSRC) at Belle Chasse developed by Allison et al., (2012). The use of Belle Chasse (RM 73) data to set up the boundary condition at RM 66 thus implies that effect of Mid-Breton diversion (RM 68) is not considered in this study. The cross-section averaged concentrations of sand and fines in the MR were specified in the model by dividing the sediment load by the discharge. The concentrations of silt and clay were specified as 75% and 25% of the total fines, respectively. The total sand was divided into 30% of 250 μ (medium sand), 37.5% of 125 μ (fine sand) and 32.5% of the 83 μ (very fine sand) median diameter size class fractions based on analysis done for the MBSD. The van Rijn (1993) sediment transport formulation is used for non-cohesive (sand) transport. The Partheniades-Krone (1965) formulation is used for modeling cohesive (silt and clay) erosion and deposition.

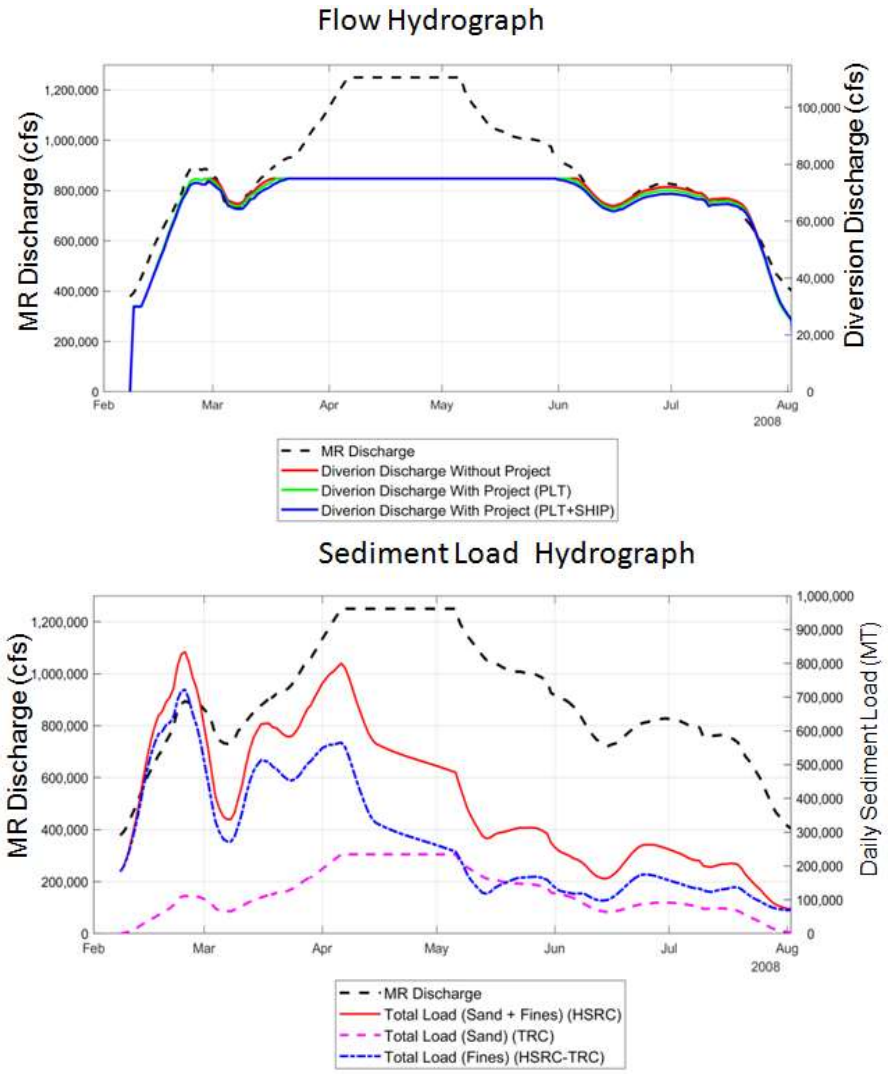

Figure 3.8. Flow and sediment load hydrographs for the 2008 diversion operation period.

Figure 3.9 shows the downstream Q-H relation used in the model. This relation is obtained by weighted averaging of the water level data over the last 10 years (2008-2018) from gages upstream and downstream of this location. The upstream is the USACE Alliance gage at RM 62.5 and the downstream gage is the USACE West Pointe a la Hache gage at RM 48.7.

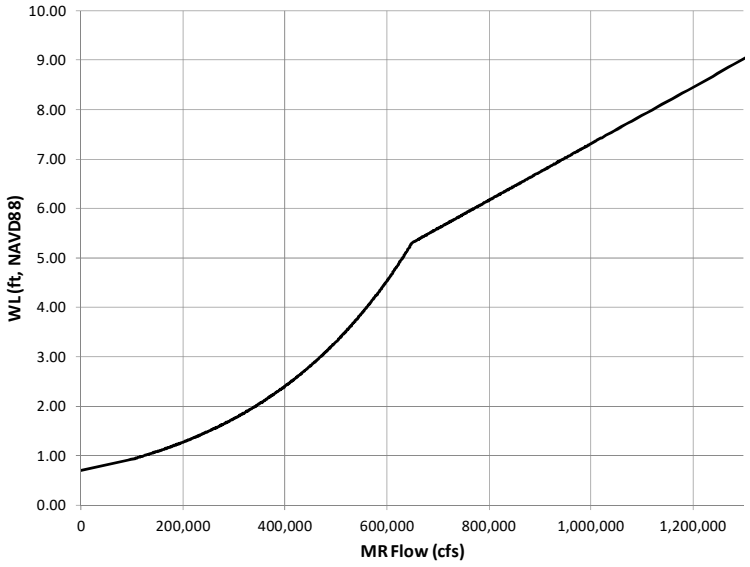

Figure 3.9. Q-H relationship used for the downstream (RM 56) boundary condition.

3.4.2 Model Setup

Figure 3.10 shows the setup of the FTN2Comp Delft3D model in 3D mode used for this study. As shown in the figure, similar to FLOW-3D, porous plates are used to model the PLT Dock barge deflector and the access way structures. Unlike FLOW-3D, Delft3D only allows for definition of porous plates along the grid directions (ξ, η represent curvilinear grid directions) at the center of a cell. The drag is quantified as a momentum sink terms in the horizontal grid directions in the momentum balance equation. The momentum loss terms for a porous plate are given by the following equations (Deltares, 2018):

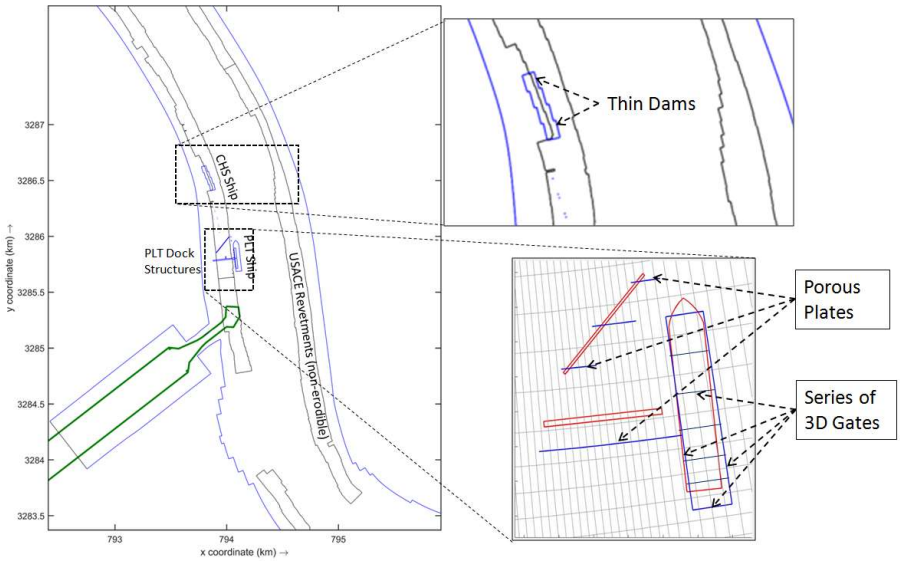

Figure 3.10. FTN2Comp (3D) Delft3D model setup for CHS Ship, PLT Dock and PLT Ship representations.

$$M_\xi = -\frac{c_{loss-u}}{\Delta x} u\sqrt{u^2+v^2},$$
$$M_\eta = -\frac{c_{loss-v}}{\Delta y} v\sqrt{u^2+v^2},$$

In the above equations, $c_{loss\text{-}u}$ and $c_{loss\text{-}v}$ are calibration coefficients and for simplicity they are considered to be the same for this study. The value of this coefficient will be calibrated to match FLOW-3D results for diverted discharge, water level, and velocities. The velocities in the X and Y directions are u and v respectively and the grid spacing is represented as Δx and Δy.

Thin dams are used to represent the effect of the CHS ship, assumed to be anchored to the river bed. The CHS dock structure was not found to be needed to be resolved due to the effects at CHS being already captured by the anchored ship unlike in the FLOW-3D model.

A series of 3D gates, placed in both grid directions and forming a rectangular floating body were used to represent the ship at PLT. The gate depth extended down to the third sigma layer from the water surface and the gate sill was located at an elevation of roughly -20 to -25 ft, NAVD88 over the hydrograph based on the variable water level and local depth. This treatment was found reasonable as the mean draft of the ship is 28 ft and meant that the bottom of the ship would vary between ~-19 ft (-28 ft draft + ~9 ft, NAVD88 WL at 1.25M cfs) and ~-25.5 ft

(-28 ft draft + ~2.5 ft, NAVD88 WL at 450K cfs) over the hydrograph. The 2D FTNOMBA model used a 2D barrier, covering the entire water depth and with a calibrated coefficient for the quadratic loss term, similar to the porous plate, instead of the 3D gates.

The diversion sediment capture efficiency is quantified by two main factors:

1. Total sediment load diverted, with particular emphasis on the sand load component of the total diverted sediment load
2. The Cumulative Sediment Water Ratio: Cumulative Sediment Water Ratio (CSWR) is defined in consistence with the past studies done by CPRA and is expressed as (Liang et al, 2017),

$$\text{CSWR} = \frac{Cumulative\ Sediment\ Load\ Diverted\ in\ the\ Diversion\ Channel \Big/ Cumulative\ Sediment\ Load\ in\ the\ River}{Cumulative\ Water\ Discharge\ Diverted\ in\ the\ Diversion\ Channel \Big/ Cumulative\ Water\ Discharge\ in\ the\ River}$$

$$= \frac{\int_{t=0}^{T} Instantenous\ Sediment\ Load\ Diverted\ in\ the\ Diversion\ Channel(t) \Big/ \int_{t=0}^{T} Instantenous\ Sediment\ Load\ in\ the\ River(t)}{\int_{t=0}^{T} Instantenous\ Water\ Discharge\ Diverted\ in\ the\ Diversion\ Channel(t) \Big/ \int_{t=0}^{T} Instantenous\ Cumulative\ Water\ Discharge\ in\ the\ River(t)}$$

The CSWR is calculated for each (n^{th}) sediment class as well as for the total sediment load.

$$\text{CSWR}_{\text{total}} = \frac{\int_{t=0}^{T} \sum_{n=1}^{N} Instantenous\ Sediment\ Load\ Diverted\ in\ the\ Channel\ (t) \Big/ \int_{t=0}^{T} \sum_{n=1}^{N} Instantenous\ Sediment\ Load\ in\ the\ River\ (t)}{\int_{t=0}^{T} Instantenous\ Water\ Discharge\ Diverted\ in\ the\ Diversion\ Channel\ (t) \Big/ \int_{t=0}^{T} Instantenous\ Water\ Discharge\ in\ the\ River\ (t)}$$

Figure 3.11 shows the reference planes used for the CSWR calculations. The MR Reference Plane: Upstream records the river sediment loads as well as volume of water passing. The Mid-Channel Plane records the diverted sediment loads and volume of water diverted.

The CSWR can be calculated for the entire 1-year hydrograph or for specific range of MR discharges (e.g., every 100,000 cfs) within the hydrograph depending upon the quantity of interest. For example, while the annual CSWR provides an estimate of the net efficiency during a representative year, the CSWR calculated over several intermediate ranges of MR discharges provides insight into the variation of the sediment capture efficiency with the various flows within a hydrograph.

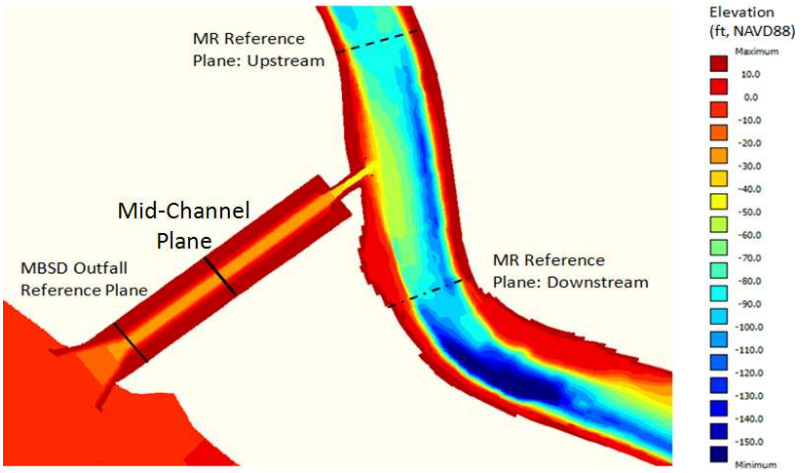

Figure 3.11. Location of reference planes for SWR and CSWR. For the SWR or CSWR computations from the FTN2Comp (3D) Delft3D model, the *Mid-Channel Plane* is used for computation of *diverted* water volume and sediment load while the *MR Reference Plane: Upstream* is used for the *MR* water volume and sediment load. Discharge rating curve from FTNOMBA (2D) Delft3D model is generated from data collected at the MBSD Outfall Reference Plane and the MR Reference Plane: Upstream.

3.5 Model Scenarios

Table 3.5 shows the model scenarios performed using the Delft3D (3D) model. The Delft3D model runs with the FTN2Comp model were run under three difference scenarios for each of the three Without- and With-Project Conditions. Five underlying stratigraphy layers were defined for all the runs. The first set (Runs 3, 4 and 5) for diversion open scenarios were conducted with no morphology change (non-erodible bed) but with bed composition update active, representative of short term (intra-annual) scale river effects when the bed level is not known to change much. The purpose is to understand suspended sediment movement without the complexity of bed change. Note that since all the models were started after creating a live bed by running the model initially for two months at high flow (until bed composition attained a steady state) and the fact that the bed composition was active during the production run period also means that the bed can still actively exchange sediment with the suspended flow and the diverted load into the river can still have both wash load and bed material load components. The second set of runs (Runs 6, 7, and 8 for diversion open and 9, 10, and 11 for diversion closed) were run

with morphology update active (as well as bed composition update active) but with no erodible stratigraphy under the initial bed. This meant that the model could deposit and erode over the initial bed only and allowed for the variation in short term (typically a scale of few years when deposition is known to happen on the bar) bed levels and diverted sediment loads due to the erosion of deposited sediment reserves (generated at low flows) at higher flows. These model results also are able to predict deposition extent and depths in the vicinity of the PLT and the MBSD intake. The third set of runs (Runs 12, 13 and 14) were run with an erodible bed below the initial bed as well as with morphology on for the With-Project (PLT Dock + Ship) scenario only. This run was initiated with 5 stratigraphy layers made up of medium sand. The main goal of this test was to understand the possible implications of the ship on the native sand bar river response.

Table 3.5. Delft3D (3D) Model scenarios.

Run No.	MBSD Diversion Open/ Closed?	PLT Dock?	PLT Ship?	Purpose
1	N/A	No	No	Model Calibration/ Validation (2018)
2	N/A	No	No	Model Validation (2008-2011)
3	Open	No	No	Quantify sediment loads and CSWR without morphology change
4		Yes	No	
5		Yes	Yes	
6	Open	No	No	Quantify above and deposition with morphology change
7		Yes	No	
8		Yes	Yes	
9	Closed	No	No	Quantify deposition with morphology change
10		Yes	No	
11		Yes	Yes	
12	Open	Yes	Yes	Quantify erosion and deposition extents with morphology change and erodible stratigraphy
13	Closed	Yes	Yes	
14	Open	Yes	Yes (locally erodible bed)	

4.0 FLOW-3D MODEL RESULTS: WATER LEVELS AND VELOCITY

4.1 Calibration and Validation

The field survey data by CPRA/WI (Allison et al., 2018) in the MR was used for calibration and validation of the FLOW-3D model under existing conditions. The CHS ship was modeled as one solid body and the associated dock structures were modeled with three porous planes. The porosities and linear loss coefficients were adjusted during calibration. The final porous mesh planes porosity was set to 0.95 and the linear loss coefficient was set to 0.78.

Figure 4.1 shows the depth-averaged velocity profile comparisons at three transects (PP01, PP02 and PP03, see Figure 5.4 for location of transects) at MR flow of 1,060,000 cfs. The blue dashed lines show the 15% PLT project model results which are without the CHS terminal and with the upstream boundary located at RM 62.7. It is observed that the right-descending bank velocities were heavily over predicted. The near bank velocity in the current model is much improved, especially at PP01 which is immediately downstream of the CHS terminal. Figure 4.2 shows the validation results at MR flow of 617,000 cfs. The simulation results agree well with the observations.

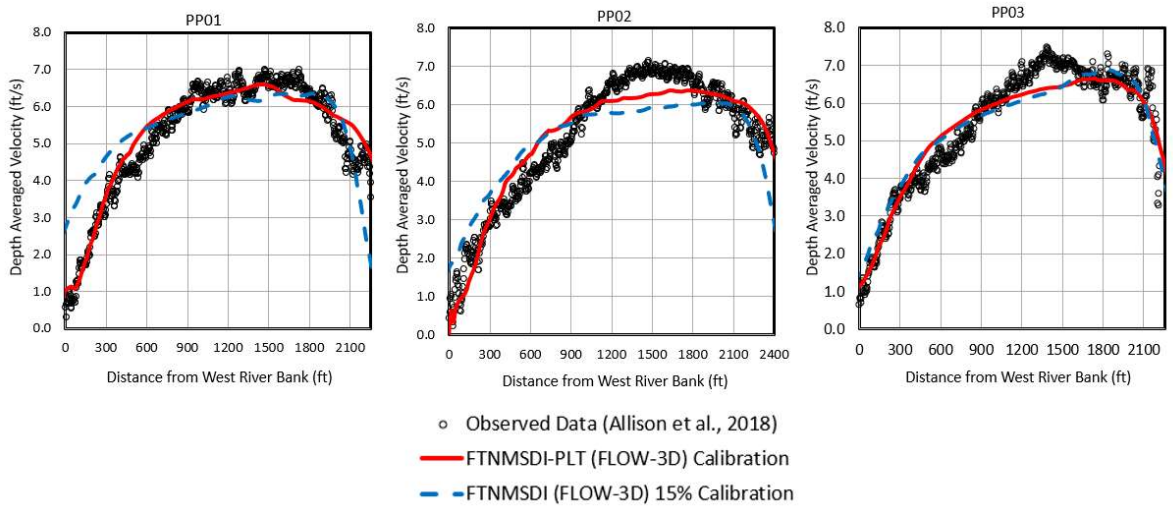

Figure 4.1. Calibration results. comparison of modeled and observed river cross-sections velocity magnitudes at three locations at MR Flow of 1,060,000 cfs.

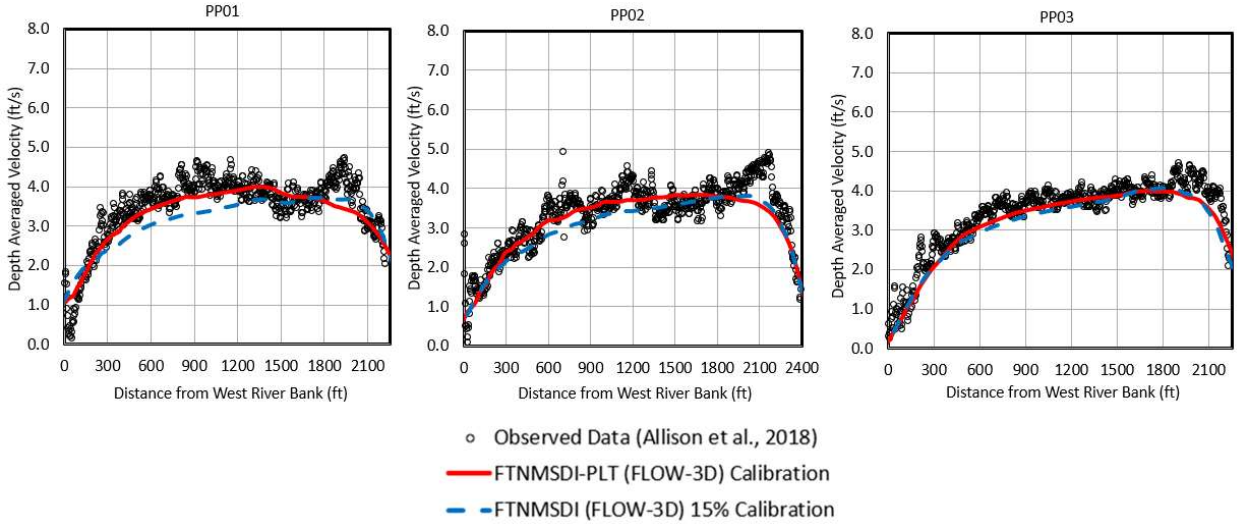

Figure 4.2. Validation results. comparison of modeled and observed river cross-sections velocity magnitudes at three locations at MR Flow of 617,000 cfs.

4.2 FLOW-3D Results: The hydrodynamic impact of PLT

Figures 4.3, 4.4, and 4.5 show the effect of the PLT dock and ship by comparing the contour plot, flow trajectories and vector plots between with and without-project cases. From the results, it is clearly seen that the existence of the PLT project changes the near-field flow dynamics around the diversion intake. The flow along the sandbar, upstream of diversion near the Right Descending Bank (RDB, looking downstream) has been disrupted. An increase in the wake region downstream of CHS was observed with the depth averaged velocity reduced by up to 2 ft/s under high flow condition. The flow trajectories show that the upstream flow streamlines pass around the PLT structure and are not able to recover to the Without-Project conditions before they reach the diversion intake. A low velocity reverse flow wake zone just downstream of the CHS structure was identified which was further influenced by the PLT project as shown on Figure 4.5. This is a potential area of deposition.

Figure 4.6 and 4.7 show the comparison of the depth averaged velocities at five transects for MR flow at 1,000,000 cfs and 600,000 cfs. In the order of the flow direction, the five transects were named PP00, PP01, PP1.5, PP02 and PP03. They are at the same locations in the 2018 survey performed by WI. From the results, it is observed that both the with-project cases are shown to have different degrees of reduction in DAV near the right descending bank. The

most significant reduction is at the transect PP1.5 which is immediately downstream of the PLT structure. For the with-PLT dock and ship case, there is about 4 ft/s reduction in DAV at high flow and 2 ft/s reduction at low flow. The reduction of DAV for the with-project cases at PP02 location is concerning since it may affect the sediment capture capabilities of the diversion by reducing the sediment transport potential. Also, DAV values falling below 3 ft/s may induce sand deposition at high flows when the river sand concentration is generally high. The PP03 location seems to have the least impact from the PLT project since it is farthest from the PLT location. By comparing the two figures, at the lower MR flow, the PLT project seems to have less impact.

Figure 4.8 and 4.9 show the depth-averaged velocity, water surface elevation and total energy head along the bank line for high flow and low flow scenarios for with and without-project cases. Consistent with the findings from Figure 4.6 and 4.7, the depth-averaged velocity has been reduced along the bank line by the addition of the PLT project. In addition, the water surface elevation and total energy head also show significant reduction caused by the PLT project. The less head available near the diversion may also cause issues with the diversion discharge.

Figure 4.10 and 4.11 shows the centerline plots of depth-averaged velocity, water surface elevation and total energy head for MR flow at 1,000,000 cfs and 600,000 cfs for the without-project case, the first with-project case (PLT dock only) and the second with-project case (PLT dock and ship). As mentioned earlier, the two with-projects cases show less total energy head available at the start of the U-Frame.

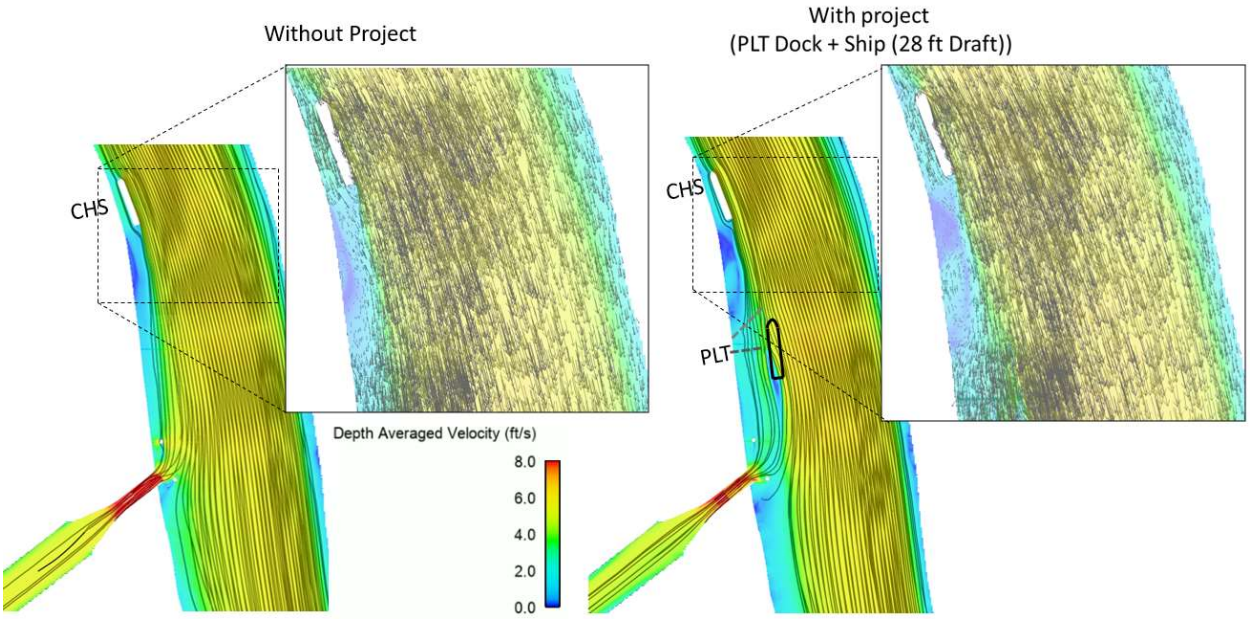

Figure 4.3. Comparison of the depth-averaged velocity contours, flow trajectories and vector plots between without-project case and with-project case (PLT dock and ship) at high flow (1,000,000 cfs).

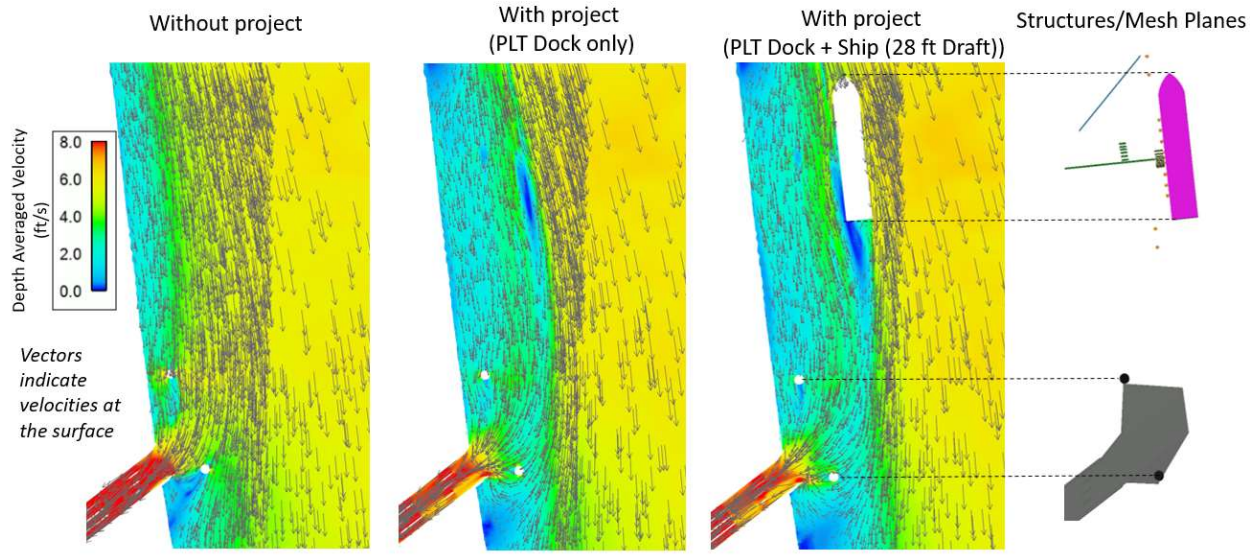

Figure 4.4. Close-up of flow-field near the diversion intake. Comparison of the depth-averaged velocity contours and vector plots between without-project case and with-project case (PLT dock and ship).

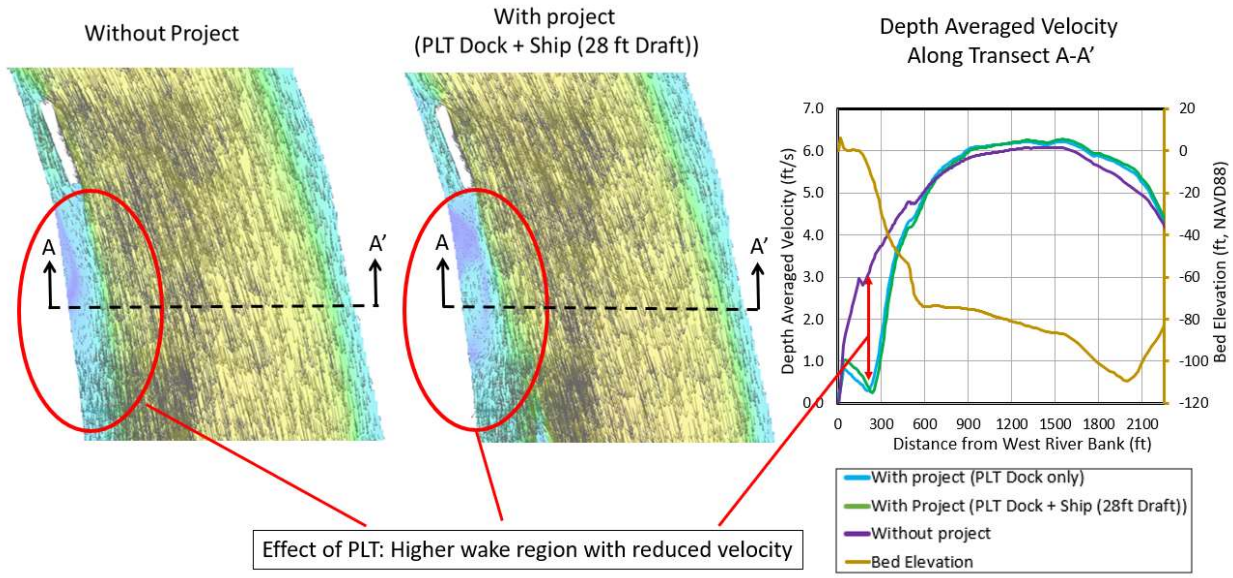

Figure 4.5. Hydrodynamics downstream of CHS and upstream of PLT: Comparison of the depth-averaged velocity profiles (right panel) at high flow (1,000,000 cfs) at transect PP00 (location on Figure 4.6) for the without-project case. The left and mid-panels show the corresponding flow patterns.

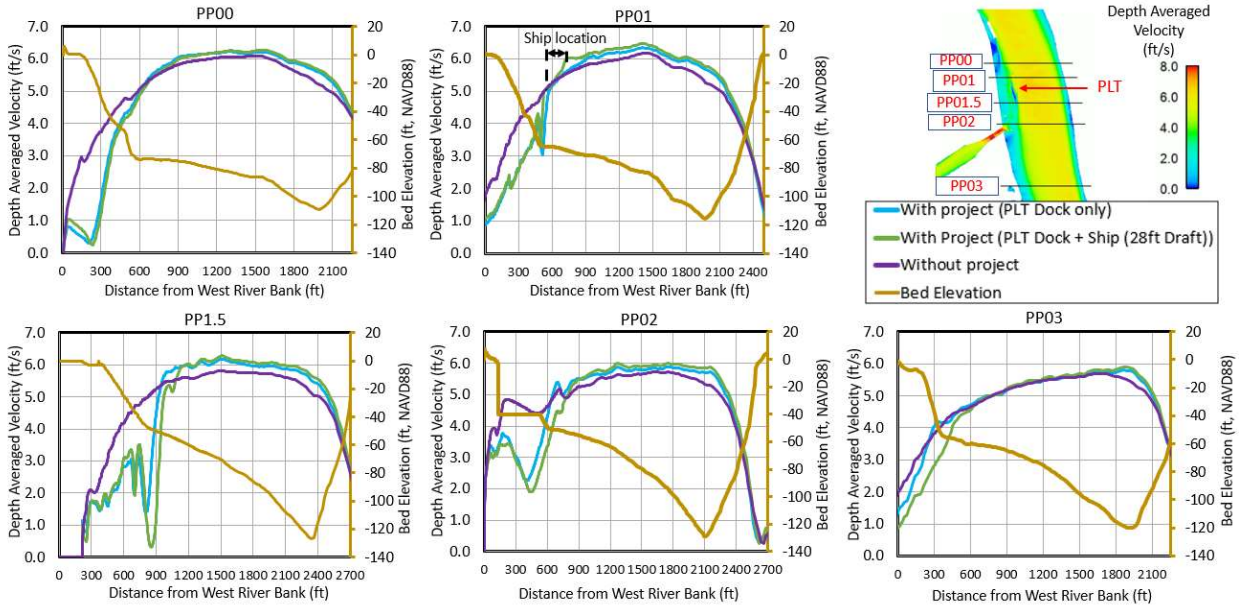

Figure 4.6. Comparison of the depth-averaged velocity profiles between With- and Without-Project conditions are shown at MR flow of 1,000,000 cfs at five transects marked in the top right inset.

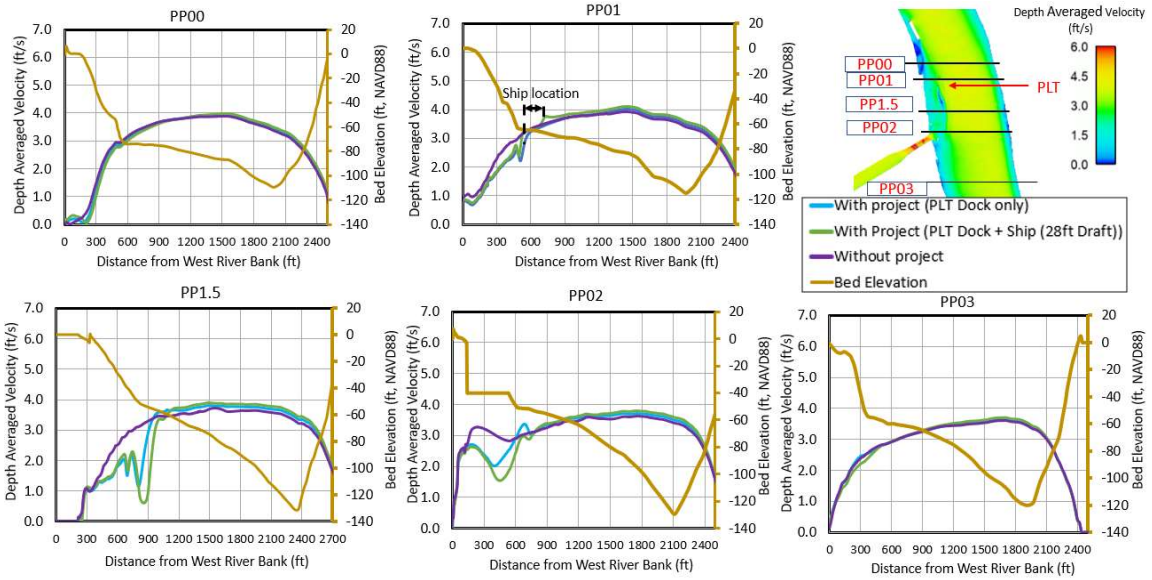

Figure 4.7. Comparison of the depth-averaged velocity profiles between With- and Without-Project conditions are shown at MR flow of 600,000 cfs at five transects marked in the top right inset.

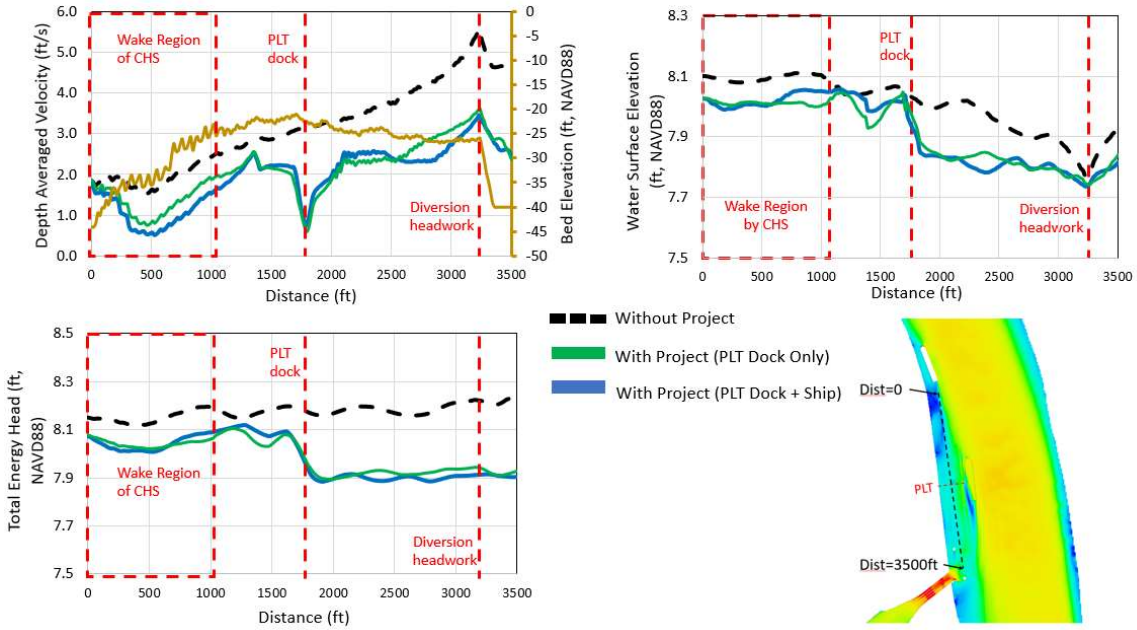

Figure 4.8. Comparison of depth-averaged velocity, water surface elevation and total energy head at MR flow 1,000,000 cfs the along a transect aligned with the RDB (inset bottom right) for the with and without-project cases.

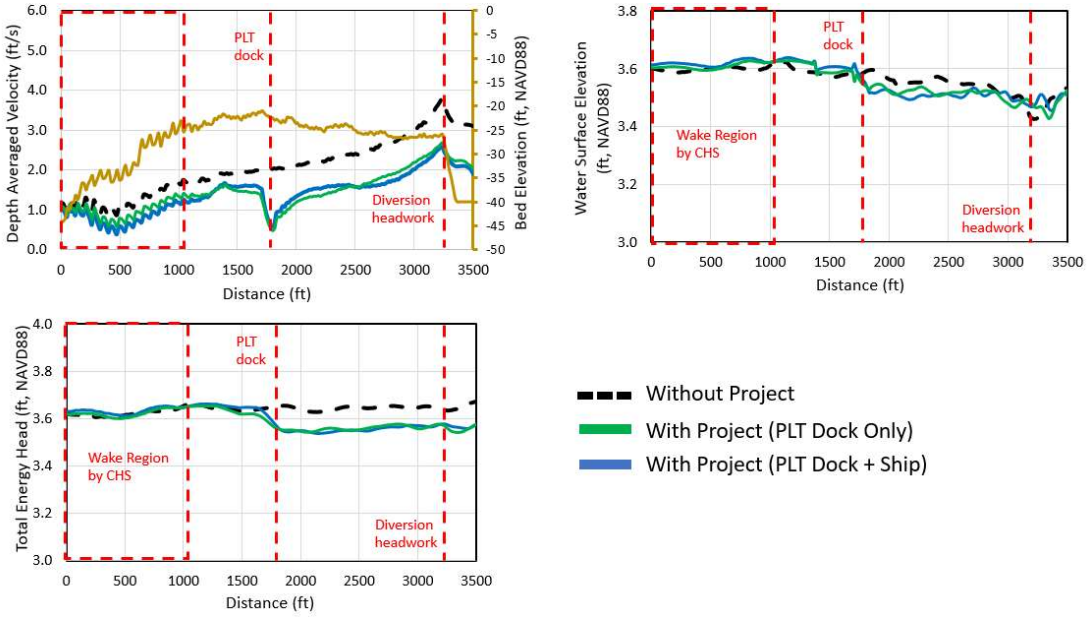

Figure 4.9. Comparison of depth-averaged velocity, water surface elevation and total energy head at MR flow 600,000 cfs the along a transect aligned with the RDB (inset bottom right) for the with and without-project cases.

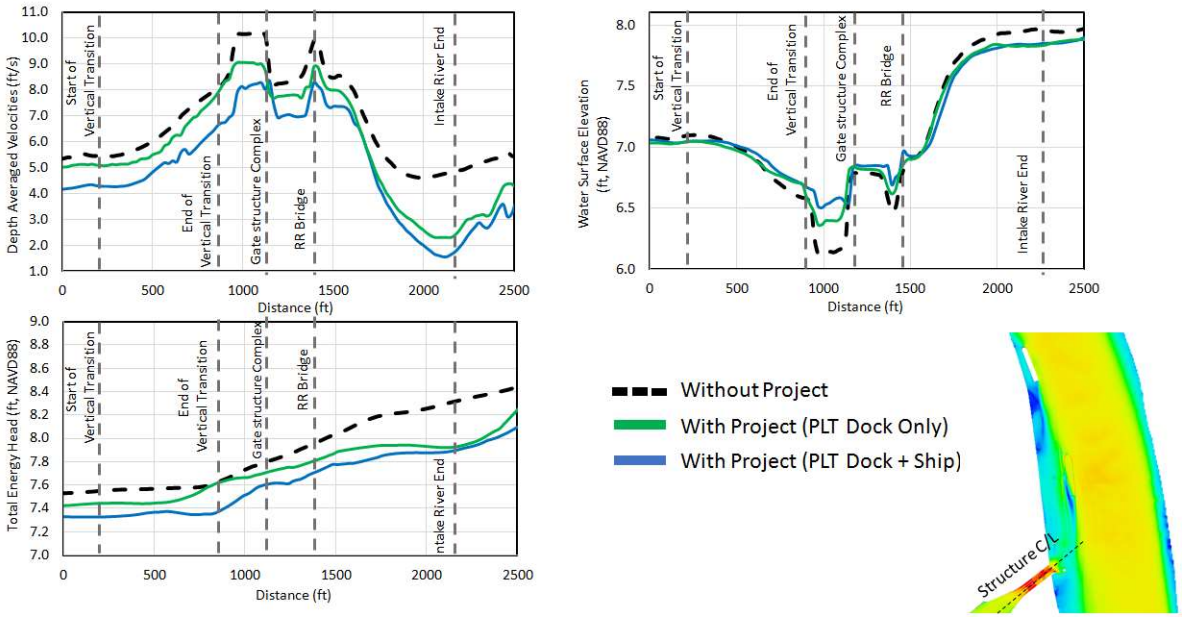

Figure 4.10. Centerline plots (line shown in inset bottom right figure) of depth-averaged velocity, water surface elevation and total energy head through the MBSD intake headworks, for MR flow 1,000,000 cfs for With- and Without-Project conditions.

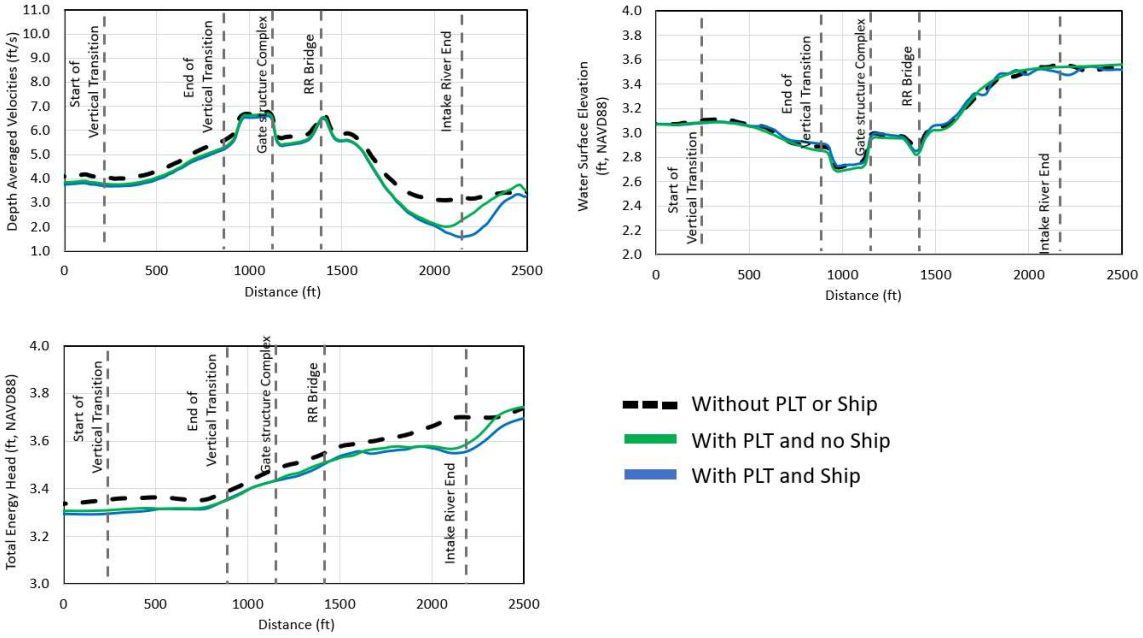

Figure 4.11. Centerline plots (along the same line as shown in inset of Fig. 4.10) of depth-averaged velocity, water surface elevation and total energy head through the MBSD intake headworks, for MR flow 600,000 cfs for With- and Without-Project conditions.

5.0 DELFT3D MODEL RESULTS

5.1 Delft3D Calibration/Validation with observed data

Extensive calibration and validation of the hydrodynamics and sediment transport model for the FTNMS (3D) Delft3D model, which is the river domain in the FTN2Comp (3D) Delft3D model (i.e., without the diversion, PLT Dock and Ship), under current conditions was conducted for the MBSD efforts. The sediment transport model was calibrated for the 2018 MR survey period and again re-validated for the 2008-2011 period. Only important figures from the MBSD modeling relevant to the current study are presented here as information to the reader.

Figure 5.1 shows the location of the sediment and velocity sampling locations in the MR survey conducted in the 2008-2011 period (Allison, 2011). The model calibration and validation for the vertical profiles for the velocity magnitude are shown on Figures 5.2 and 5.3. Overall the model results are within the acceptable range of error in the field observations and match the velocities at the RDB (near the proposed diversion) well.

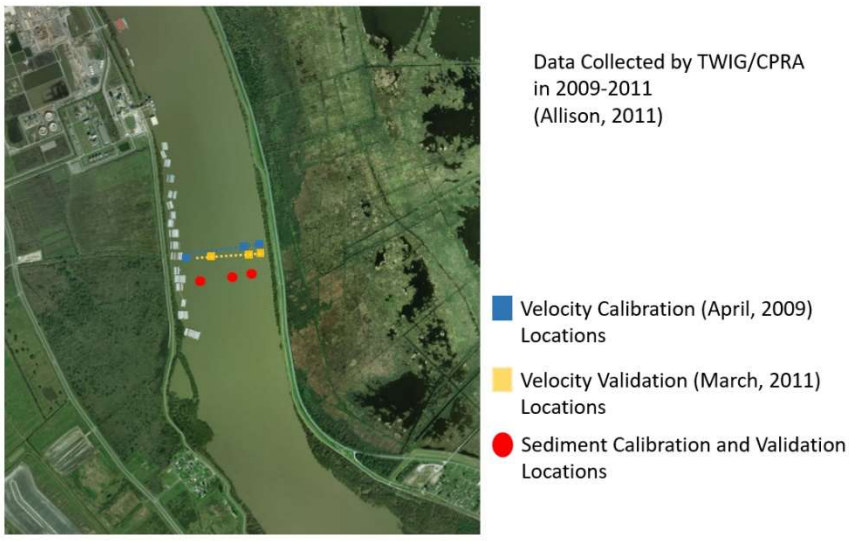

Figure 5.1. Velocity and sediment sampling locations for the 2008-2011 MR survey (Allison, 2011).

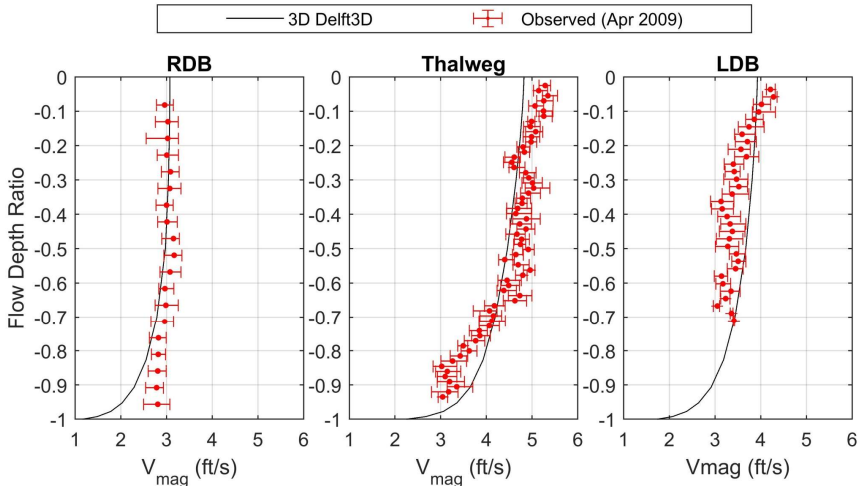

Figure 5.2. Model calibration (Apr 2009 event, MR flow 742,000 cfs): Velocity profiles compared with field observations from CPRA's 2008-2011 MR survey, at the three locations shown on Figure 5.1.

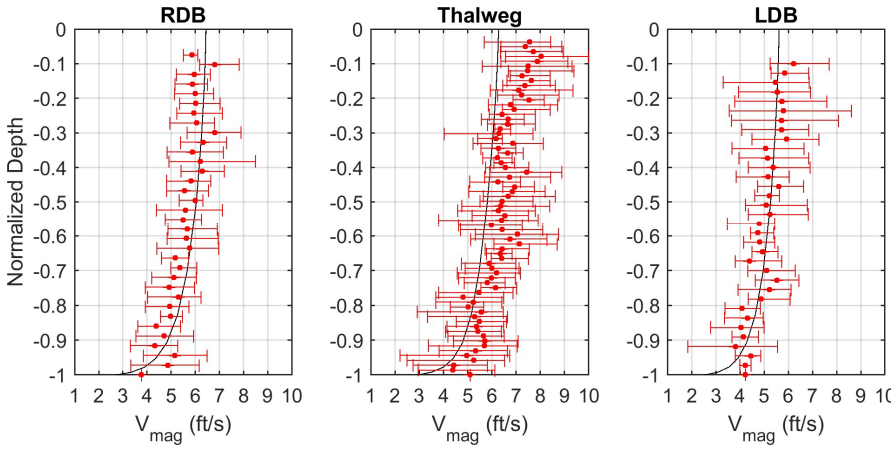

Figure 5.3. Model validation (March 2011 event, MR flow 966,000 cfs): Velocity profiles compared with field observations from CPRA's 2008-2011 MR survey, at the three locations shown on Figure 5.1.

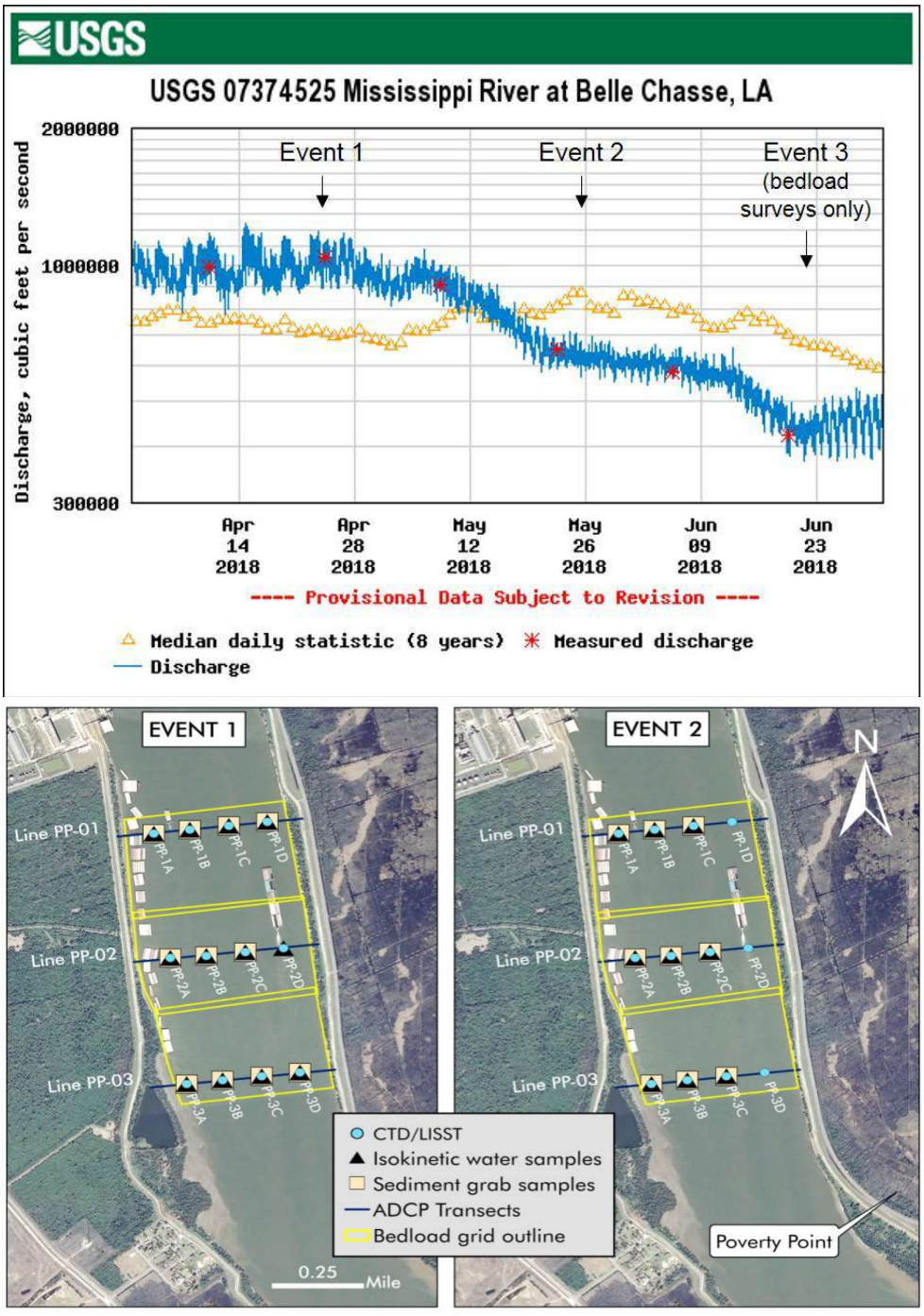

Figure 5.4. Top Panel: 2018 MR Survey Events. Bottom Panel: 2018 MR Survey cross-sections and sediment survey locations (figures reproduced from Allison et al., 2018).

The MR survey conducted in 2018 revealed the need to include the CHS terminal effects on the velocity near the proposed PLT location (PP-01) on Figure 5.4, particularly at the high flow (~1,000,000 cfs) event (Event 1). The model was revised to include the CHS terminal and model results for cross-sectional velocity distribution as shown on Figure 5.5.

The hydrodynamics and sediment transport model were originally calibrated and validated for two events (2009 and 2011). After additional data was available in 2018, the model was re-calibrated and re-validated for the 2018 period, including the effect of the CHS terminal. The comparison of the total sediment (sand) load with observed data for the 2018 period are shown on Figure 5.6 and for the 2008-2011 period on Figure 5.7.

Vertical profiles of suspended sand and fines concentration compared with observed data for the 2009 and 2011 events are shown on Figures 5.8 and 5.9. For the 2018 period the vertical profiles of suspended sand concentration are compared with observed data as on Figures 5.10 and 5.11.

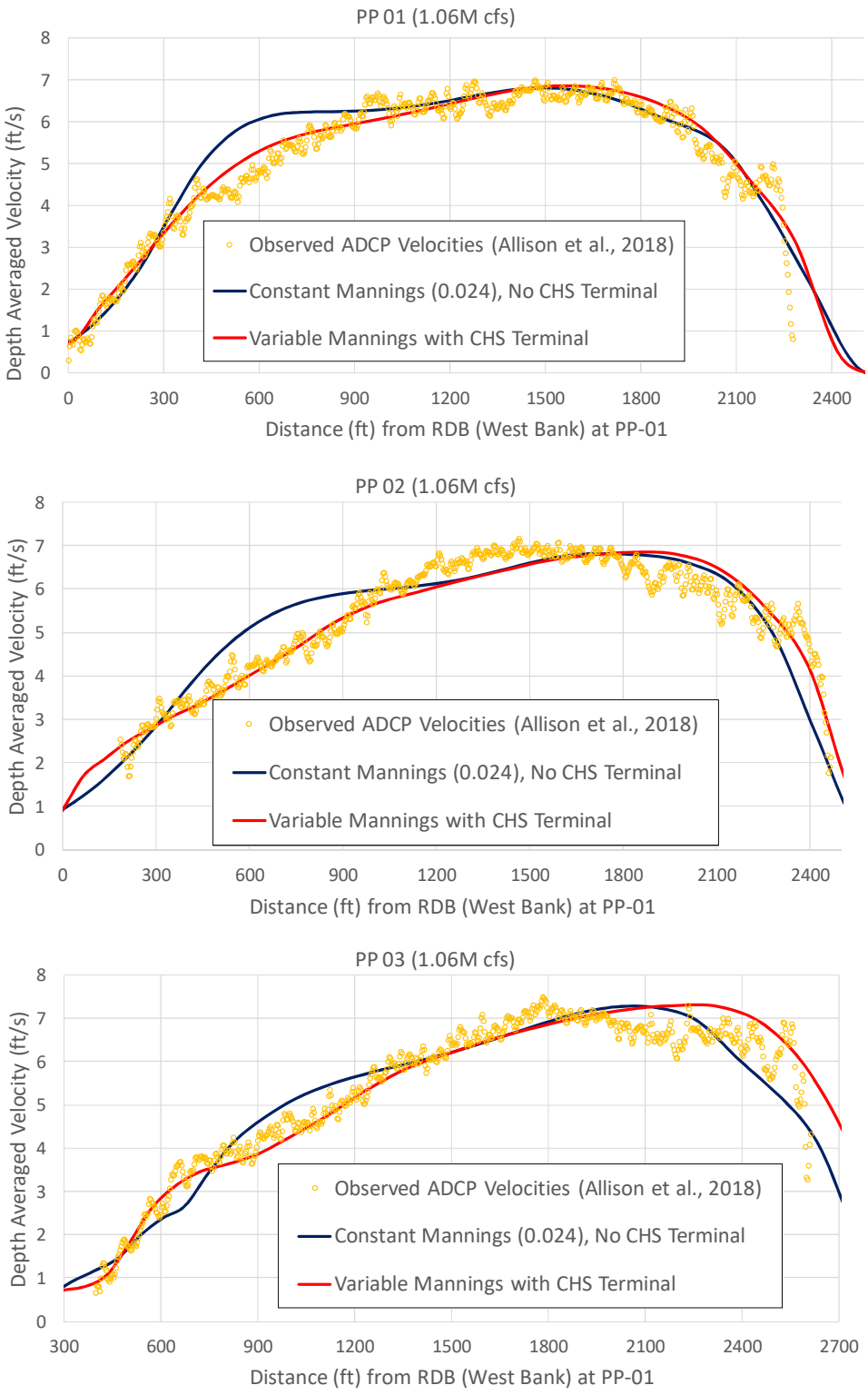

Figure 5.5. 2018 MR Survey Event 1 model results including CHS terminal shown in red line.

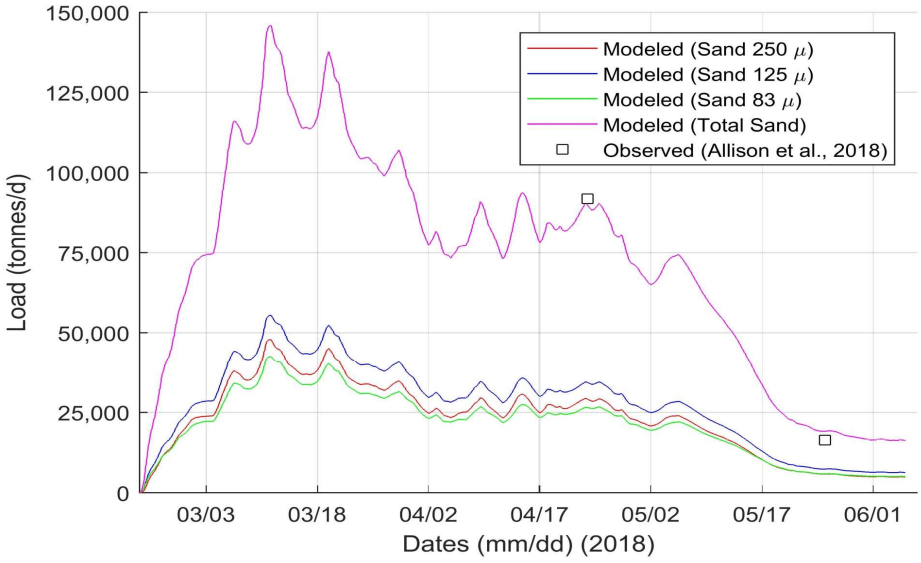

Figure 5.6. Calibration (Event 1) and Validation (Event 2) of 3D Delft3D model for total sand loads for the 2018 MR survey.

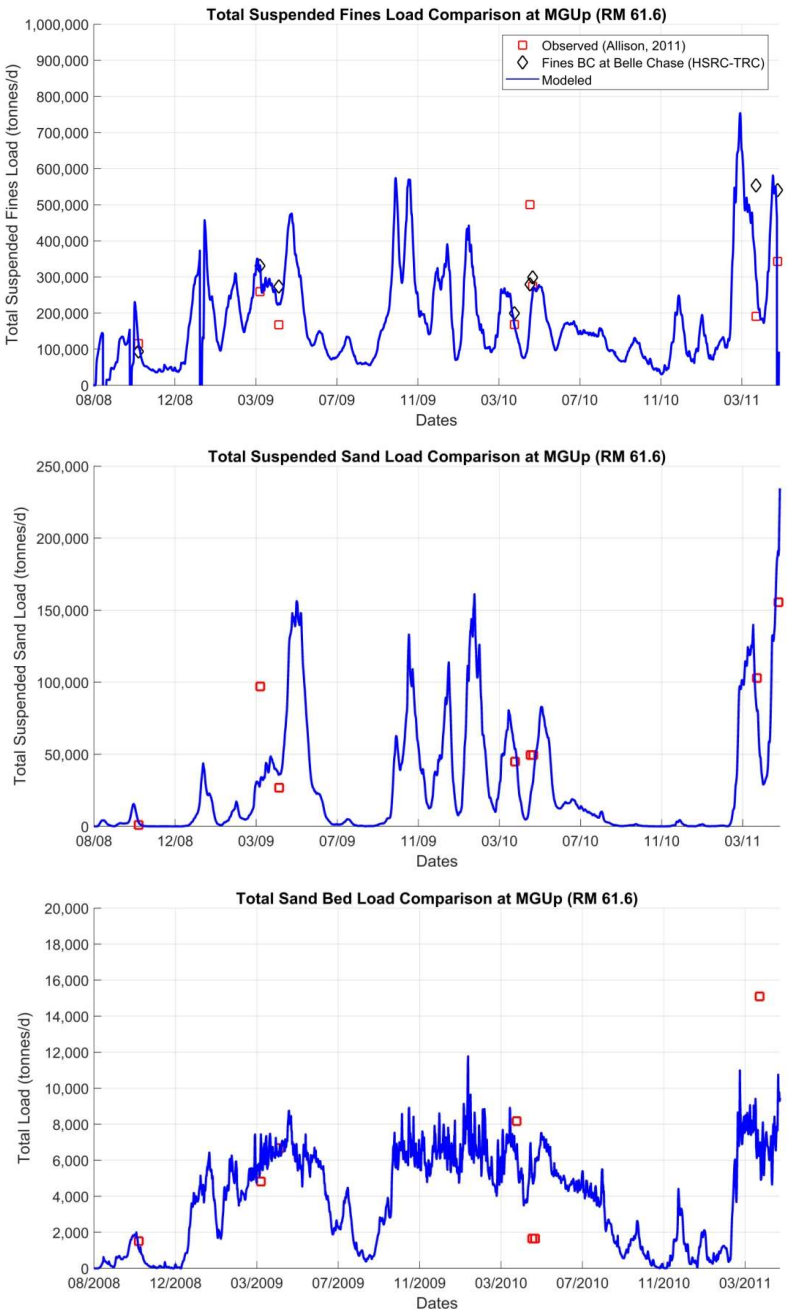

Figure 5.7: Validation of the 3D Delft3D model for the 2008-2011 period hydrograph. Comparison of modeled and observed fines (silt and clay) are shown in the top panel, suspended sand loads in the middle panel, and bed load in the bottom panel at the proposed MBSD location (RM 61.6)

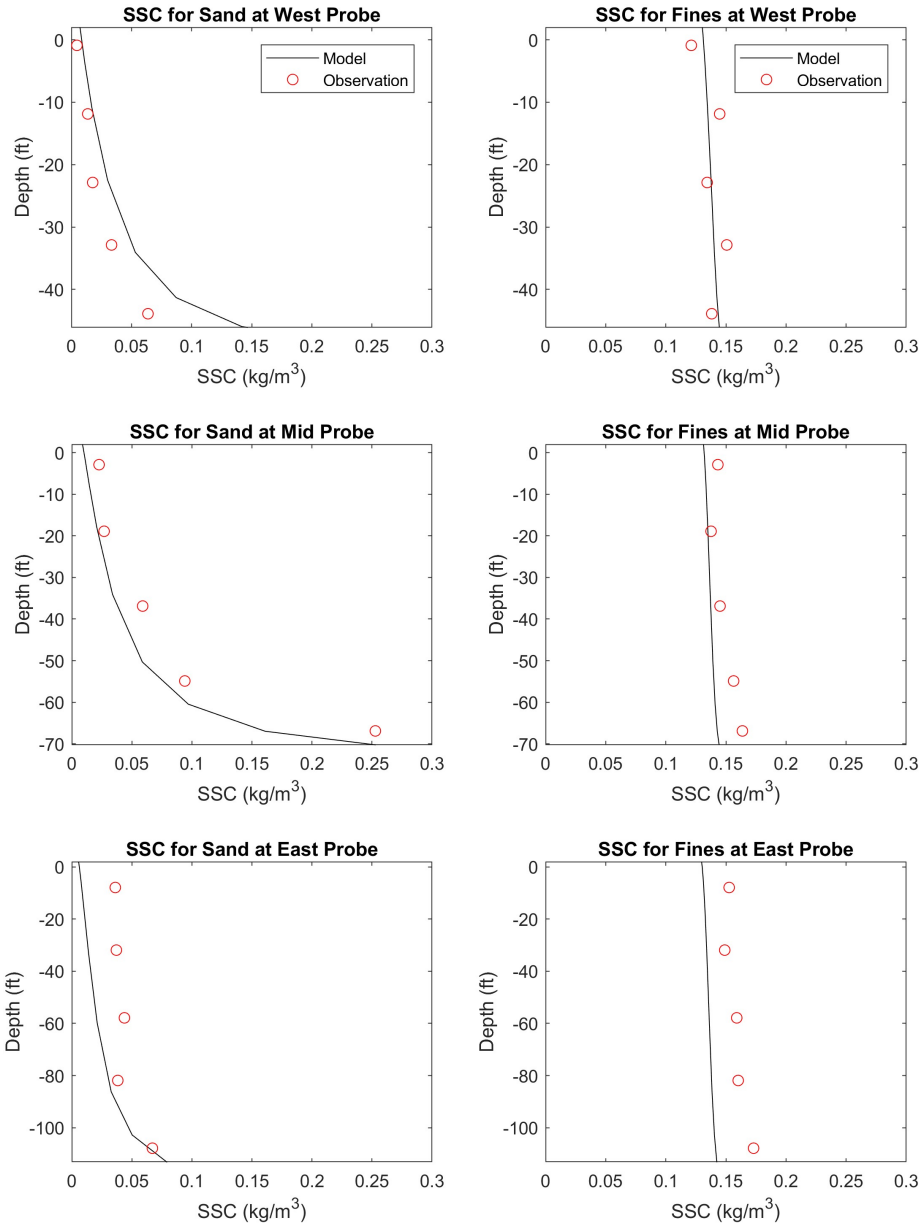

Figure 5.8. Model calibration (Apr 2009 event, MR flow 742,000 cfs): Vertical profiles of suspended sand concentration (left column) and suspended fines concentration (right panel). Probe locations shown on Figure 5.1.

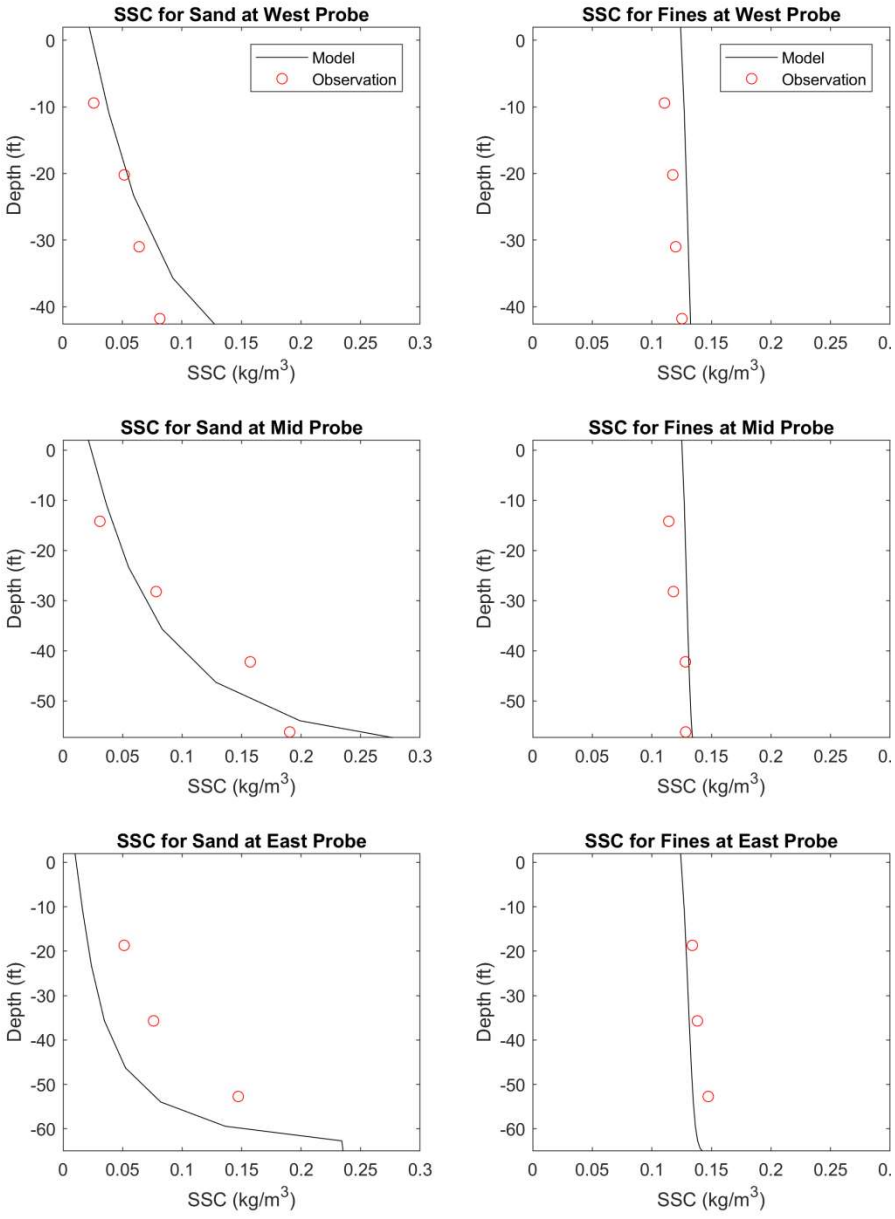

Figure 5.9. Model validation (March 2011 event, MR flow 966,000 cfs): Vertical profiles of suspended sand concentration (left column) and suspended fines concentration (right panel). Probe locations shown on Figure 5.1

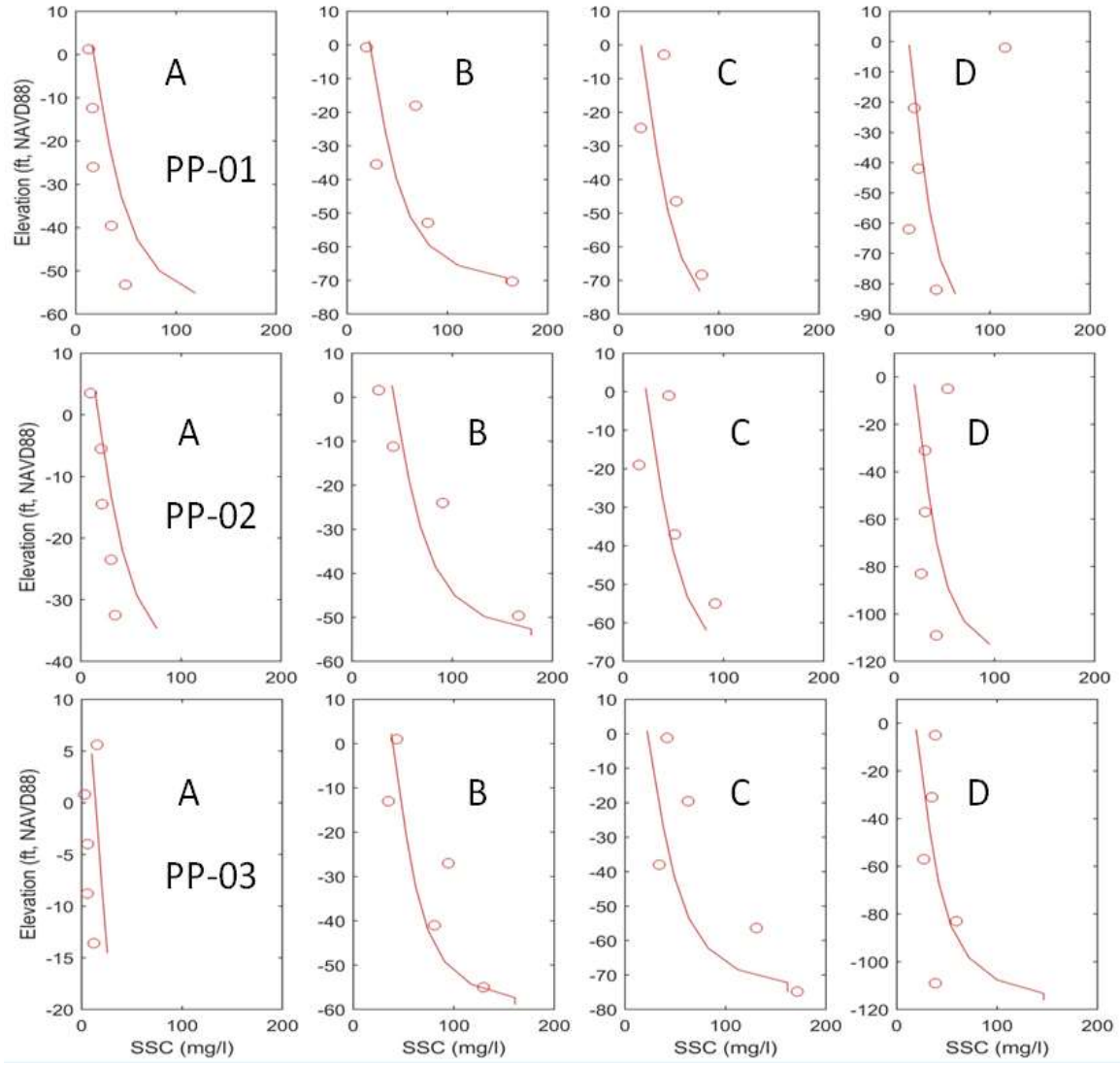

Figure 5.10. Model calibration (Event 1, 1,060,000 cfs MR flow) 2018 MR Survey: Comparison of vertical profiles of suspended sand concentration at locations marked in Fig. 5.4

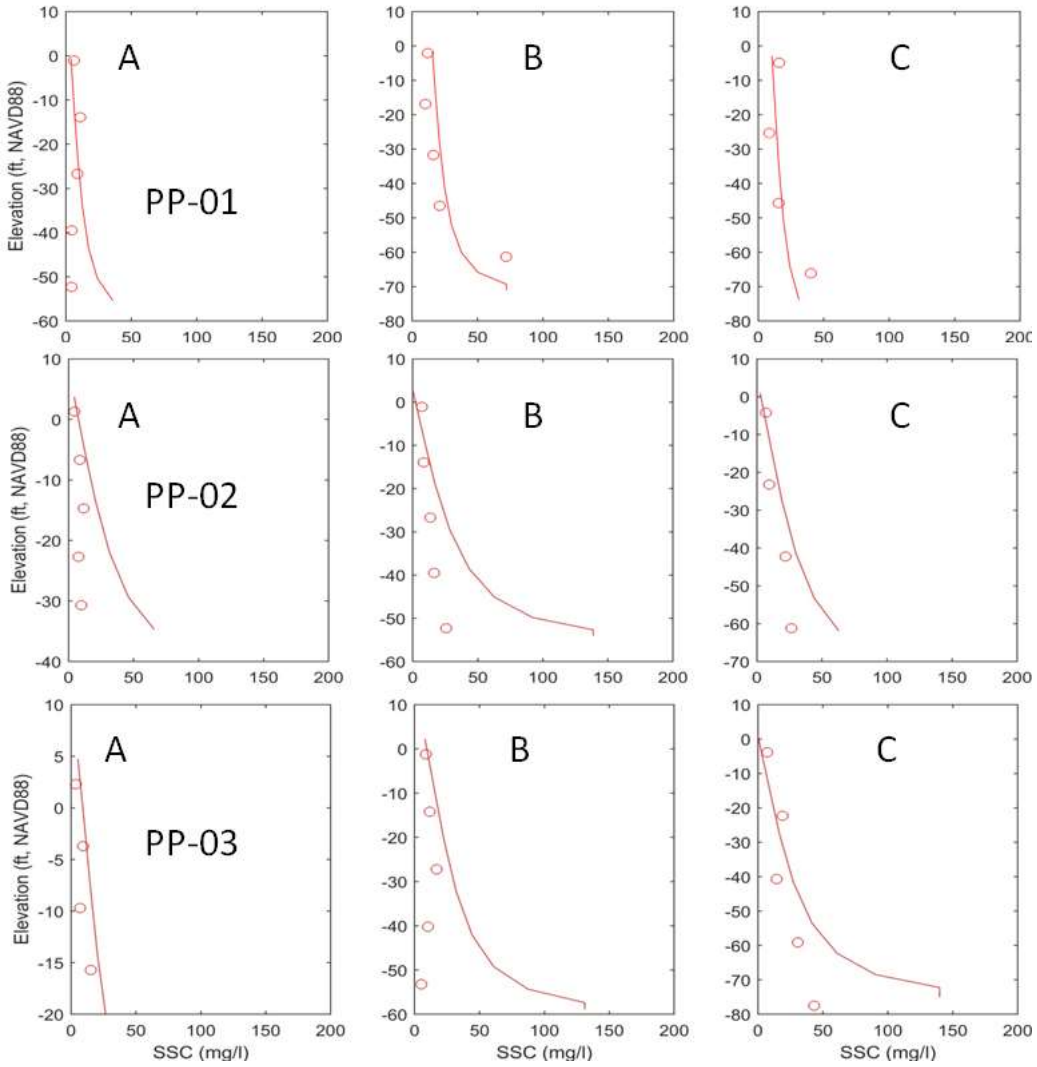

Figure 5.11. Model validation (Event 2, 620,000 cfs MR flow) 2018 MR Survey: Comparison of vertical profiles of suspended sand concentration at locations marked in Fig 5.4.

Figure 5.12 shows the comparison of modeled and observed cross-sectional contour plots of suspended sand concentrations at the three locations surveyed in 2018 (Figure 5.4). As seen from the figure, the 3D Delft3D model simulates the spatial distribution of the sand across the river section on the sand bar relatively well when compared to the observed data.

The calibrated FTNMS model is used to setup the FTN2Comp Delft3D model used for the PLT study and subsequently is calibrated with FLOW-3D model results as described in the following sections.

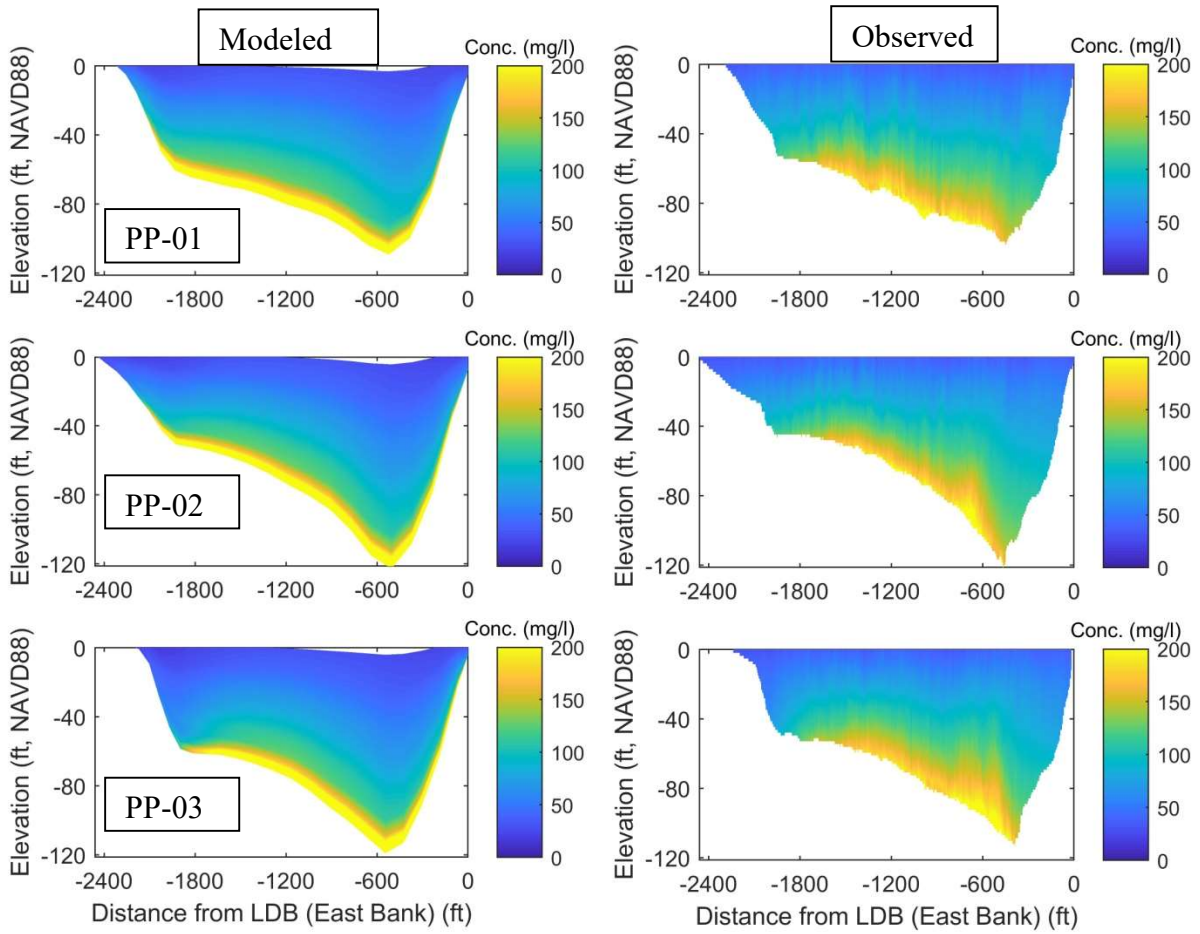

Figure 5.12. Comparison of modeled sand concentration with observed values at the three locations PP01, PP02 and PP03 for Event 1. The observed values were obtained from backscatter data of the ADCPs.

5.2 Delft3D Calibration with FLOW-3D

Table 5.1 shows the comparison of Delft3D FTN2Comp model predicted diverted discharge with the FLOW-3D FTNMSDI results. The boundary conditions for the two models were the same and the only value calibrated was the coefficients (C_{loss}) of the porous plates representing the PLT Dock structure. For simplicity all the plates were set to have the same coefficient as it was found that variation of coefficient values between the plates affected little the velocity and discharge at the diversion intake. A calibrated value of 0.9 in the Delft3D model matched well both the diverted discharge as well as the water level, depth-averaged velocity and total energy head profiles (shown later in Figs 5.13-5.15 from the Delft3D model with the FLOW-3D model.

Figures 5.13 (Without-Project), 5.14 (with-project, PLT Dock only) and 5.15 (With-Project, PLT Dock + Ship) show the comparison of Delft3D FTN2Comp and FLOW-3D FTNMSDI model profiles after calibration of the porous plate coefficients. Water Level (WL) (upper panel), the Depth-Averaged Velocity (DAV) (mid-panel) and the Total Energy Head (TEH) (bottom panel) were compared along two transect locations as shown in the bottom of Figure 5.13.

Table 5.1. Comparison of calibrated Delft3D model diverted discharge with the FLOW-3D model along with calibration coefficients tested. A value of 0.9 was selected which gave the best comparison with the FLOW-3D diverted discharge.

Case	MR Flow (cfs)	Diverted Discharge (cfs)		Percent Difference in Delft3D discharge from FLOW-3D (%)	FTN2Comp Delft3D Calibration Coefficients (C_{loss})
		FLOW-3D	Delft3D	FLOW-3D-Delft3D /FLOW-3D x 100%	Porous Plates (PLT Dock)
Without-Project	1,000,000	74,900	74,000	+1.2	-
With-Project (PLT Dock Only)	1,000,000	67,400	73,300	-8.7	0.1
With-Project (PLT Dock + Ship)	1,000,000	66,500	72,300	-8.8	0.1
Without-Project	1,000,000	74,900	74,000	+1.2	-
With-Project (PLT Dock Only)	1,000,000	67,400	69,600	-3.0	0.7
With-Project (PLT Dock + Ship)	1,000,000	66,500	68,700	-3.3	0.7
Without-Project	1,000,000	74,900	74,000	+1.2	-
With-Project (PLT Dock Only)	1,000,000	67,400	67,100	+0.5	0.9
With-Project (PLT Dock + Ship)	1,000,000	66,500	66,000	+0.8	0.9
Without-Project	1,000,000	74,900	74,000	+1.2	-
With-Project (PLT Dock Only)	1,000,000	67,400	66,100	+2.0	1.2
With-Project (PLT Dock + Ship)	1,000,000	66,500	64,500	+3.0	1.2

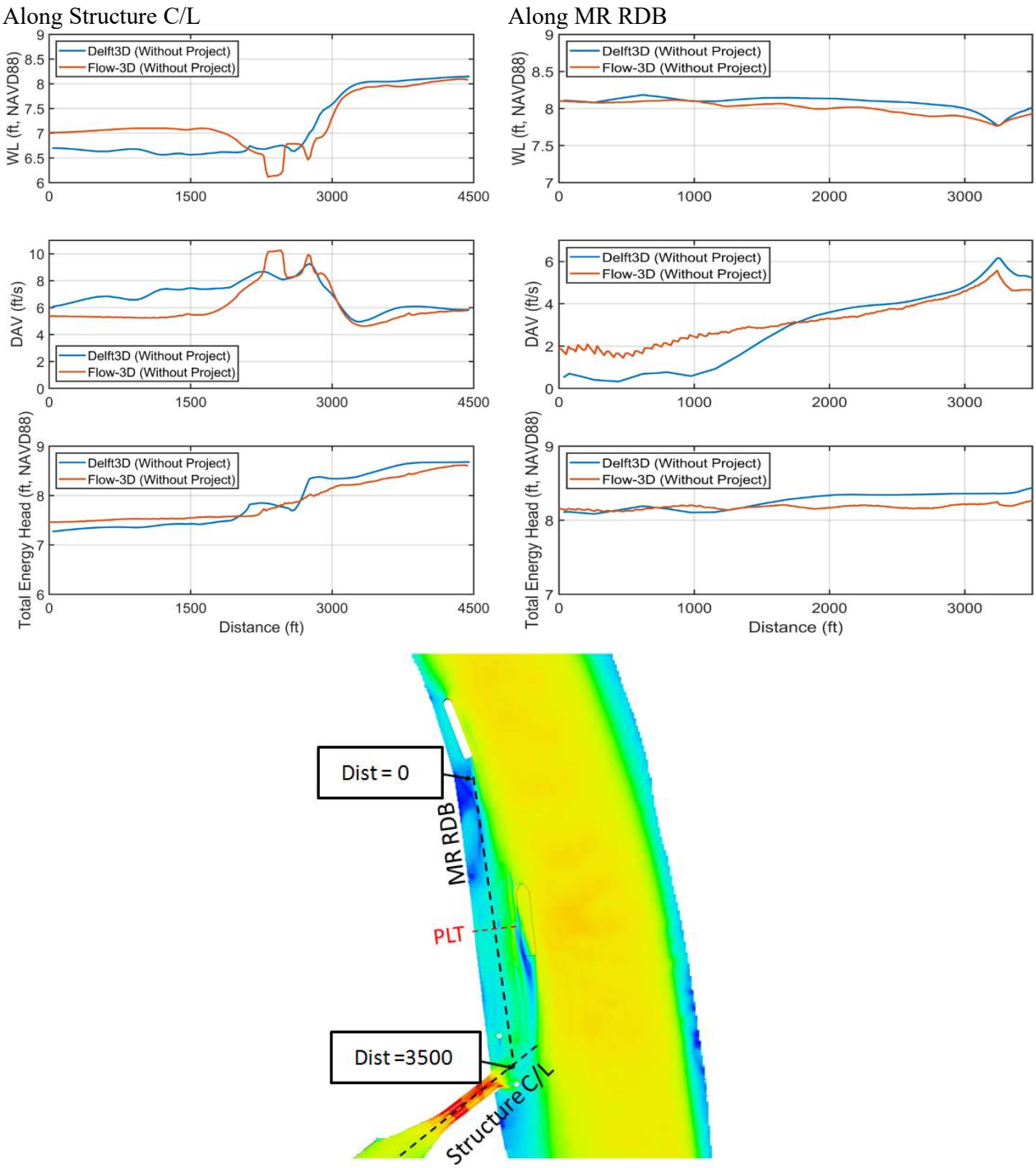

Figure 5.13. Without Project: Delft3D FTN2Comp (3D) and FLOW-3D FTNMSDI modeled water level, depth-averaged velocity and total energy head comparisons along two lines, along the RDB and the structure centerline (shown in bottom). MR Flow is 1,000,000 cfs.

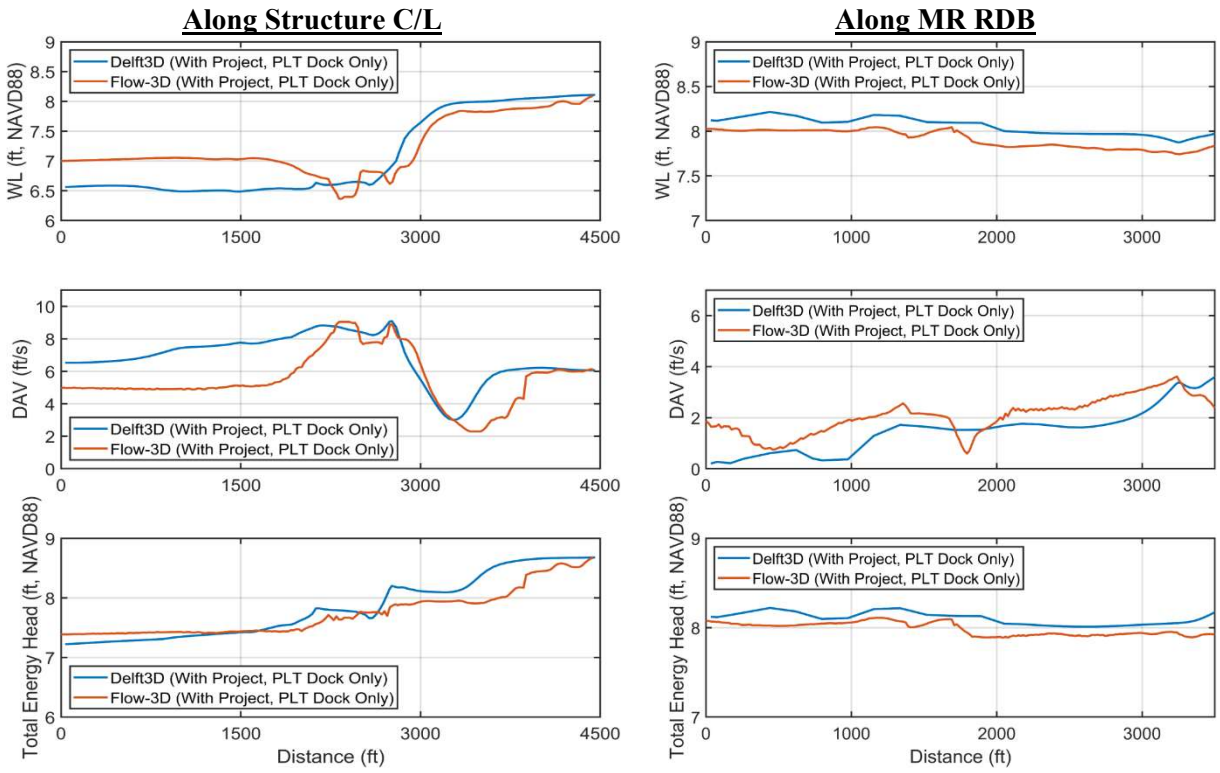

Figure 5.14. With-Project (PLT Dock Only): Delft3D FTN2Comp (3D) and FLOW-3D FTNMSDI modeled water level, depth-averaged velocity and total energy head comparisons along two lines, along the RDB and the structure centerline (same locations shown as in bottom of Figure 5.1). MR Flow is 1,000,000 cfs.

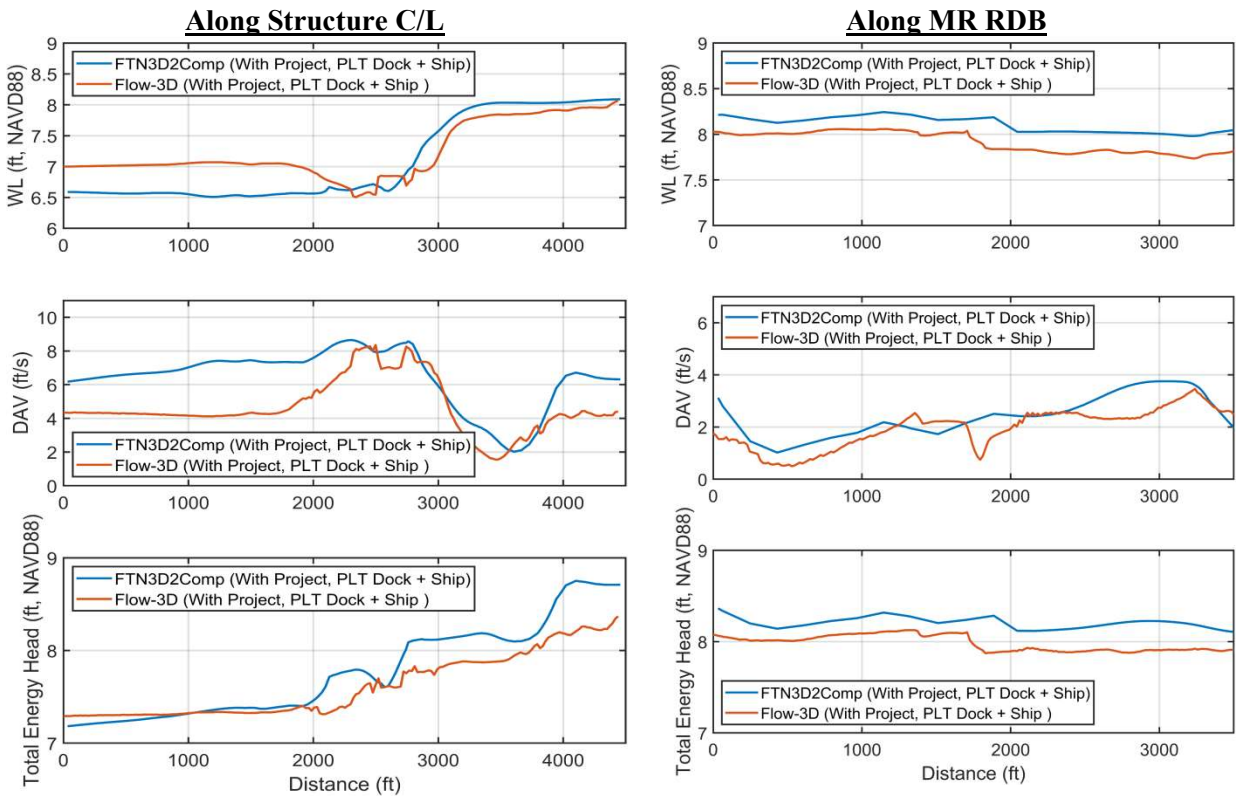

Figure 5.15. With-Project (PLT Dock + Ship): Delft3D FTN2Comp (3D) and FLOW-3D FTNMSDI modeled water level, depth-averaged velocity and total energy head comparisons along two lines, along the RDB and the structure centerline (same locations shown as in bottom of Figure 5.1). MR Flow is 1,000,000 cfs.

Figure 5.13 shows comparison of Delft3D and FLOW-3D model profiles after calibration along the structure centerline and along the RDB. The bottom figure shows the location of the lines along which the model results were compared, one along the Mid-Barataria Sediment Diversion (MBSD) structure centerline (C/L) and another along a line passing roughly parallel to the river along the RDB starting about 3,500 ft upstream of the intake C/L and ending at the intake. These two locations are chosen due to the importance of the hydrodynamics in the vicinity of the intake and the RDB where the PLT project is proposed. Note that this bottom plot is a generic figure showing the PLT Dock and Ship and is meant to simply signify the relative location of the lines with respect to project features under consideration, the specific case results shown here are from Without-Project (i.e., no PLT Dock or Ship) conditions. Overall both the models predict similar water level and DAVs. One of the differences observed in the models is

the zone immediately downstream of the CHS terminal where the DAVs are predicted less (~1 ft/s) in Delft3D compared to FLOW-3D (~2 ft/s).

Figure 5.14 shows the comparisons between the two models, under With-Project (PLT Dock only) of modeled WLs, DAVs and TEHs along the same line locations as on Figure 5.13. It is seen that while the overall trend between the two models match well for both water level and total energy head, some spatial variation in the velocities along the RDB is evident due largely to the different treatment of the porous planes in the two models. In general, the Delft3D model tends to slightly overpredict the water level (by < 0.25 ft) and consequently underpredict the velocities (by < 1 ft/s) along the RDB. Velocity predictions improve as one moves down the RDB towards the intake.

Figure 5.15 shows the comparison between the two models under With-Project (PLT Dock + Ship) condition. The profiles agree well within the two models with consistent variations shown in Figures 5.13 and 5.14, due to slightly different water level predictions between the models.

5.3 Delft3D Model Results: Discharge and Sediment Transport

Once the Delft3D FTN2Comp (3D) model porous plate coefficients for the PLT structure components were calibrated, the same setup was used to run the FTNOMBA (2D) Delft3D model to generate basin boundary conditions (which will later be used as input at the mid-channel location into the FTN2Comp 3D sediment model) for sediment transport modeling shown in the next section. The 3D gate representation for the ship was changed to a 2D barrier with a loss coefficient of 0.9 for the 2D model. A comparison of 2D and 3D FTN2Comp model runs with the 2D barrier representation of the ship for the former and a 3D gate for the latter, under With- and Without-Project conditions indicated that the 2D barrier representation as an acceptable form of representation of the ship dynamics in a 2D version of the model. Note that the main purpose of the 2D model is to get comparative head losses and generate mid-channel discharge boundary conditions for the sediment modeling using the FTN2Comp (3D) model; the choice of this difference has no implication on sediment modeling which is still run in the 3D Delft3D model with the 3D gate representation of the ship.

Figure 5.16 shows the comparison of With- and Without-Project condition profiles at the same two transect locations as in Figs. 5.13-5.15 from the FTNOMBA 2D model. An important aspect to note here is that this is the first time in this study that the Delft3D model was run with influence of basin conditions included (full basin modeled) and with a downstream MR Q-H relation, the interaction of the basin WL, downstream WL in the river results in a draw-down in the river which is evident as a reduced water level (~ 7.1 ft, NAVD88) in these runs versus the previous calibration runs (~8-8.1 ft, NAVD88) which were run without the basin. Note that the effect of the change in the boundary does not affect the calibration of the barrier coefficients which are intrinsic properties of the structures themselves and Reynolds number ranges (Section 3.3.2) which still remain invariant.

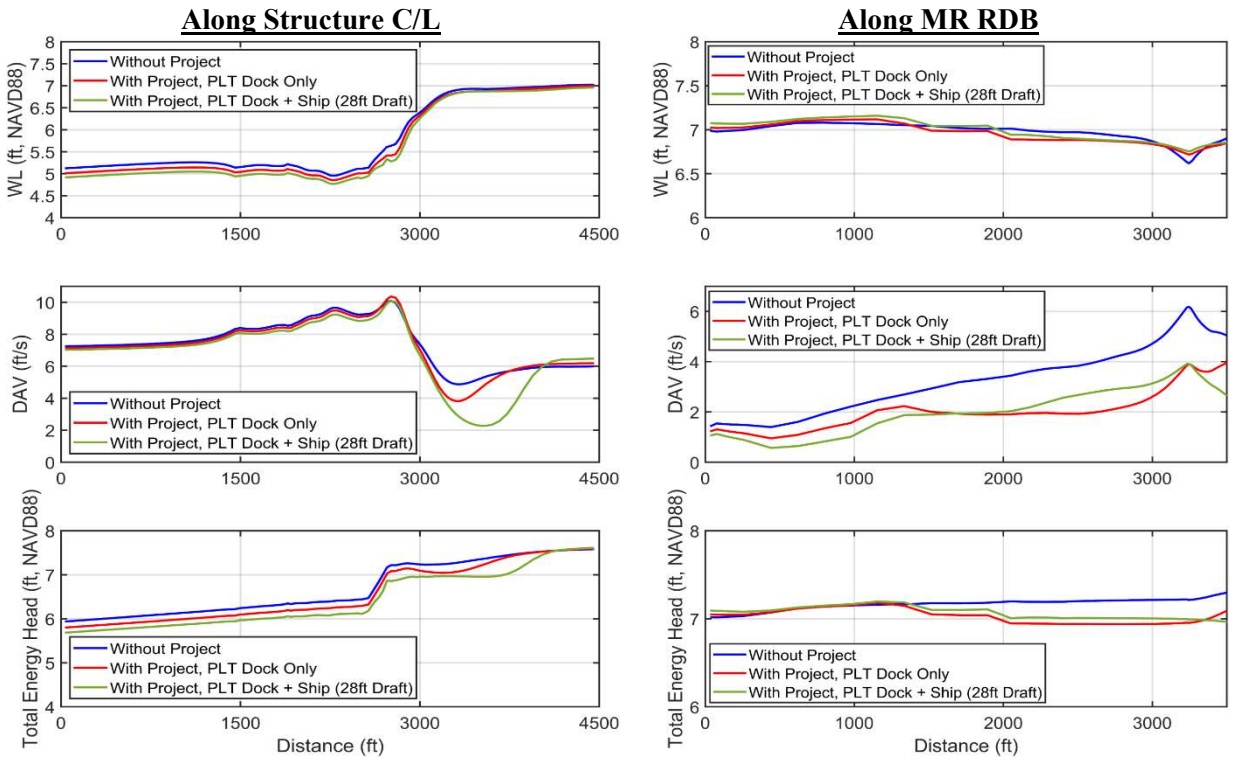

Figure 5.16. With- and Without-Project Delft3D FTNOMBA model comparisons: FTNOMBA (2D) Delft3D predicted profiles under With- and Without-Project conditions, including basin water level effects. MR Flow is 1,000,000 cfs.

To quantify the variation in diverted discharge with river discharge over a variety of river flows, for With- and Without-Project conditions, the FTNOMBA (2D) Delft3D model was run

for the 2008 hydrograph period for the interval when the river flow ranged from 450,000 cfs on the rising limb to 450,000 cfs on the falling limb (proposed operational period of diversion). The resulting Q-Q plot (MR discharge versus Diversion Discharge) is shown on Figure 5.17. Separate best fit curves are drawn between flow ranges below and above 700,000 cfs to distinguish the trends in the data. It can be seen that the reduction in diverted discharge between the With- and Without-Project conditions increase with increasing river discharge, primarily because of increasing drag losses at the PLT Dock structure and ship due to increasing river velocity with flow.

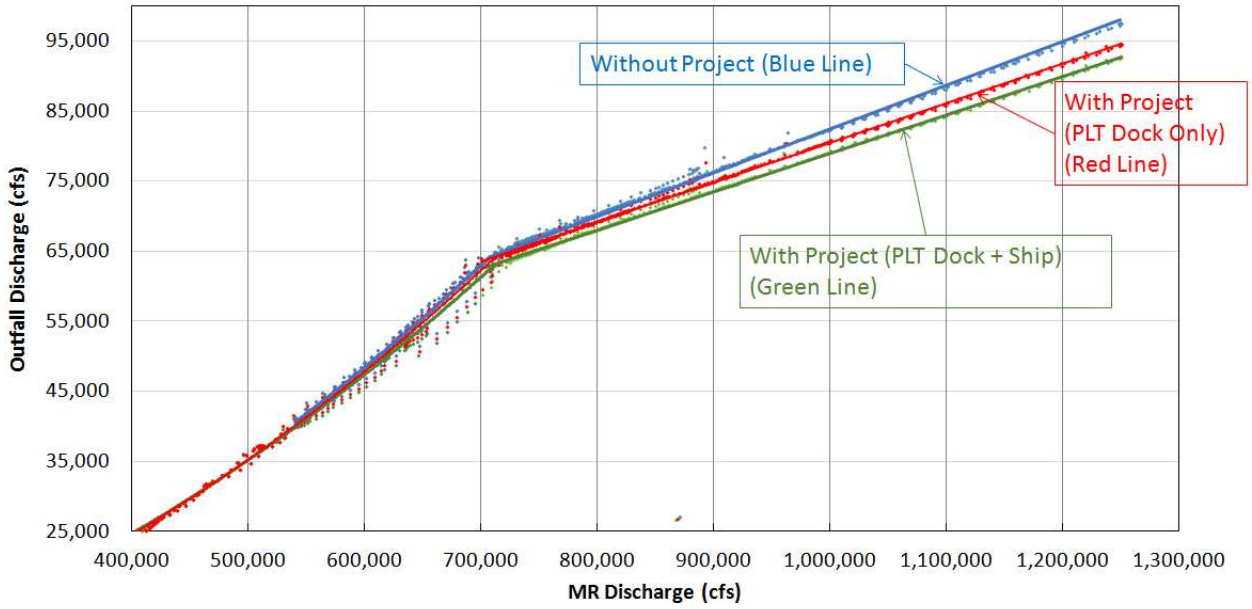

Figure 5.17. MR Discharge versus Outfall Discharge Plot for the three cases (Without-Project, With-Project –PLT Dock Only and With-Project – PLT Dock + Ship).

Table 5.2 shows the diverted discharge variation at specific MR flows (High, Medium, Low and Trigger flows) as well as the relative reduction due to the dock and the ship. At high flow, the reduction due to the PLT Dock alone is estimated to be about 2.4% and that due to the combined effect of the PLT Dock+Ship is estimated to be about 4.3%, suggesting that the additional 1.9% can be attributed due to the ship. The reduction, as noted before, decreases with decreasing river flow and is negligible at the trigger flow. Note that even though the diversion flow is shown to reach above 75,000 cfs in this table and Figure 5.17, in reality the diversion flow will be capped at 75,000 cfs using the gates. Thus, the presence of the PLT facility and the

PLT facility with the ship reduces the inlet flow capacity or the efficiency of the sediment diversion on the order of about 2 - 4 %. As a result of the reduced flow, fine sediments will be reduced somewhat proportionately, as shown later in the section, on the order of about 1 to 5%.

Table 5.2. Comparison of diverted discharge from FTNOMBA (2D) Delft3D model at Trigger (450,000 cfs), low (600,000 cfs), medium (800,000 cfs) and high (1,000,000 cfs) MR flow and relative percent reduction compared to the Without-Project scenario.

MR Flow	Without Project	With Project (PLT Dock Only)	With Project (PLT Dock + Ship, 28 ft Draft)	Percentage flow reduction due to Ship (28 ft draft) only
1,000,000 cfs (High Flow)	82,400	80,400 (-2.4%)	78,900 (-4.3%)	1.9%
800,000 cfs (Medium Flow)	69,900	69,100 (-1.2%)	67,900 (-2.9%)	1.7%
600,000 cfs (Low Flow)	48,350	47,800 (-1.1%)	47,300 (-2.2%)	1.1%
450,000 cfs (Trigger Flow)	30,000	30,000 (0%)	30,000 (0%)	0.0%

The FTN2Comp (3D) Delft3D sediment model was run using the discharge boundary conditions at the mid-channel location using the output from the FTNOMBA (2D) Delft3D model results for the same operational period of the diversion (450,000 cfs in the rising limb to 450,000 cfs in the last falling limb) for the 2008 hydrograph year. The discharge time series was capped at 75,000 cfs for the sediment runs. Figure 5.18 shows the histogram plots representing the variation in Total Sand and Fines load and SWR separately, under Without-Project (Run # 3), With-Project (PLT Dock only, Run # 4) and With-Project (PLT Dock + Ship, Run # 5) scenarios with MR flow. No morphology change is modeled in these runs. Mean values averaged over an interval of 100,000 cfs MR flow bins are plotted. The percent reduction in the sediment loads and SWR are also shown. The vertical bars (±Standard Deviation about the Mean) indicate the range of variability in the diverted sediment load and SWR due to the variation in the sediment load in the MR as a result of the hysteresis effect inherent in the fines and sand load distribution in the rising and falling limb. The sand load increases monotonically with increasing discharge with little variability while the fines load exhibits a more complex trend due to the hysteresis effect.

The percentage reduction in sand load is seen to be higher at MR flows exceeding 900,000 cfs with values ranging about ~15% due to the PLT Dock only and ~40-45% due to the combined effect of the PLT Dock and the Ship. The ship is seen to have a disproportionate additional impact on the sand load diverted. The fines load reduction is mostly less than ~5%. As a dedicated sediment diversion, whose primary purpose is to divert as much sand as possible (the fines being well distributed in the water column and are expected to be diverted with the flow anyway), the reduction in sand load was investigated further. The main reason for sand load reduction can be identified by tracking the dominant path ways of high near-bed Suspended Sand Concentration (SSC) which is the main source of the diverted sand in the river at four distinct river flows, namely, 1,250,000 cfs, 1,000,000 cfs, 800,000 cfs, 600,000 cfs and 450,000 cfs as shown on Figures 5.19 through 5.22.

Figure 5.19 shows the near-bed SSC spatial distribution along with velocity vectors under the three scenarios (Runs 3, 4 and 5 with no morphology change) at 1,250,000 cfs MR flow. A distinct bypassing effect of the high concentration RDB sand is seen under With-Project conditions as compared to that in the Without-Project. When the ship is not present, even though the dock is affecting the sand flow, sand is still able to bypass the PLT Dock and get diverted into the intake somewhat. On the other hand, when a ship is present a major percentage of the main sand plume, feeding the diversion, is now blocked either directly by the ship or is affected by its wake region. The blocked sand bypasses the diversion as mostly suspended load through two zones, a small portion between the PLT Dock and Ship and a major portion around the ship along with the main river flow bypassing the diversion, which in turn increases the concentrations slightly downstream of the diversion. This explains the disproportionate effect of the PLT Ship in reducing the diverted sand load versus the effect of the PLT Dock alone. Figures 5.20 to 5.22 show similar phenomenon with the exception that the near-bed cross-river concentration gradient along the RDB is lower at Medium and Low flows and explains the lower reduction effects seen at these flows than at the higher flows (>900,000 cfs).

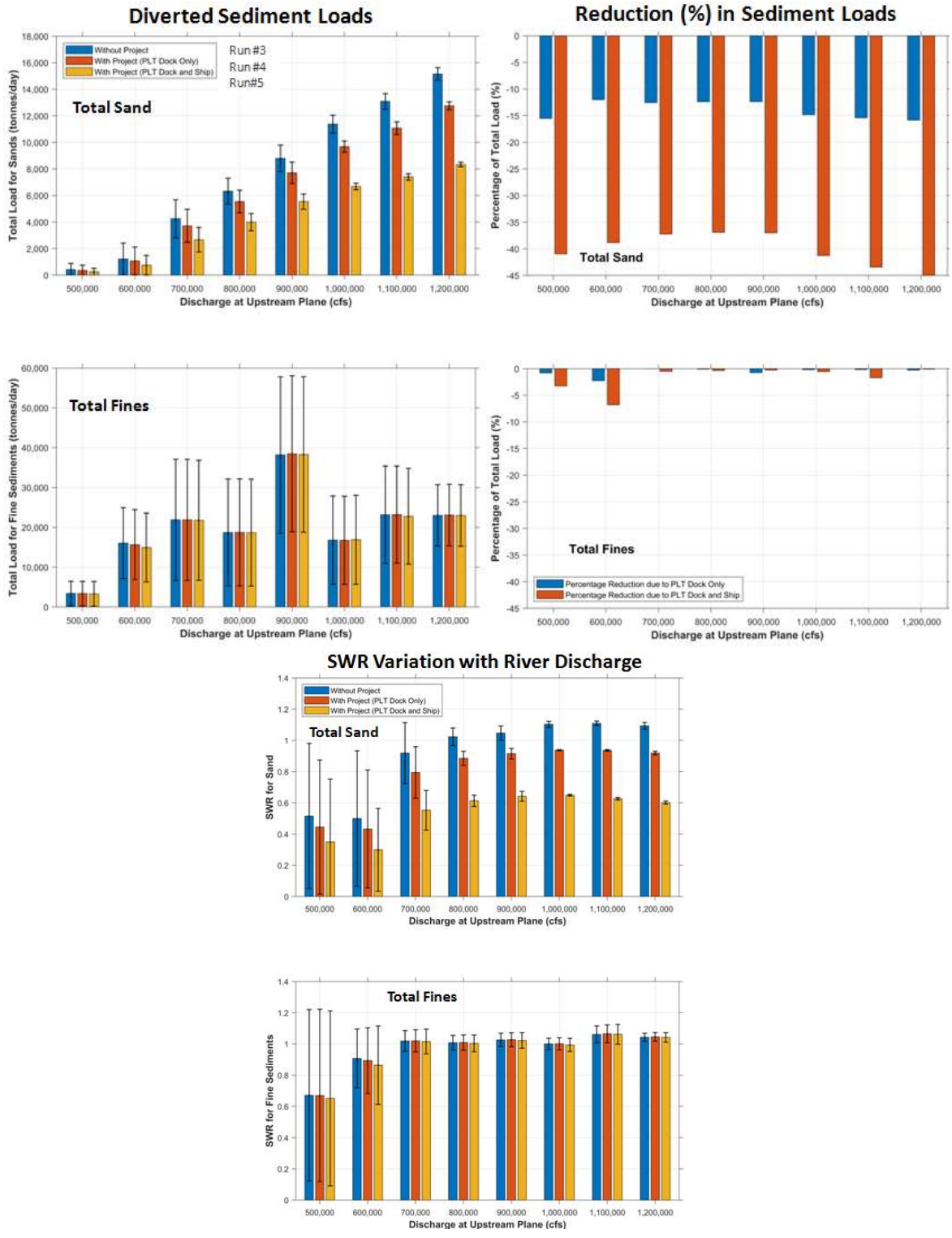

Figure 5.18. No Morphology Change (Runs 3, 4 and 5): Variation of Total Sand and Fines loads (upper left panel) and percent reduction from Without-Project scenario with MR flow. Bottom panel shows the variation in SWR of Total Sand and Fines. Model run was using the 2008 hydrograph year for the entire operational period.

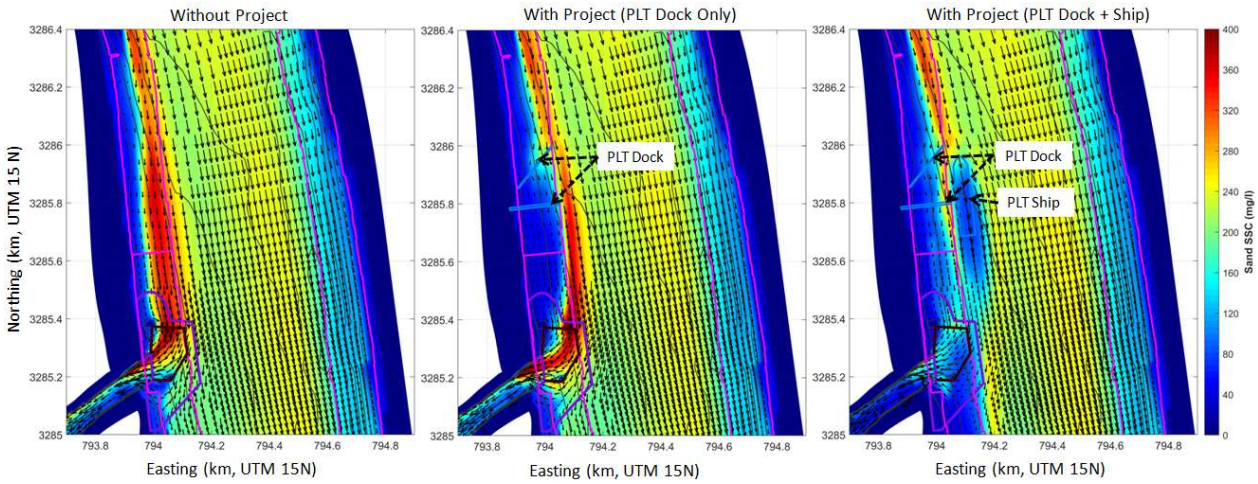

Figure 5.19. No Morphology Change: Near-bed Suspended Sand Concentration (SSC) at 1,250,000 cfs MR flow.

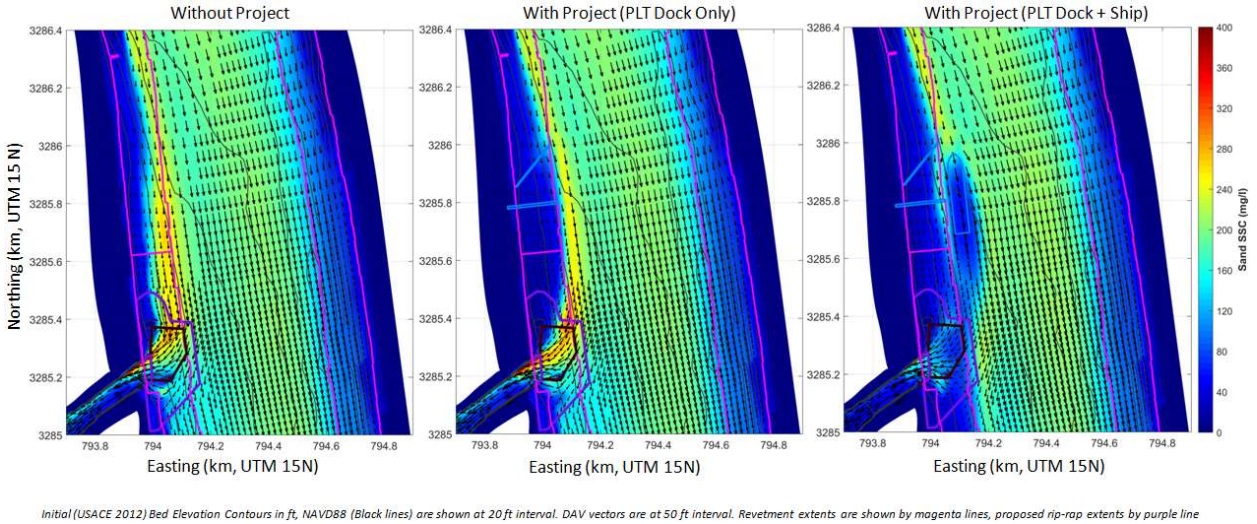

Figure 5.20. No Morphology Change: Near-bed Suspended Sand Concentration (SSC) at 1,000,000 cfs MR flow.

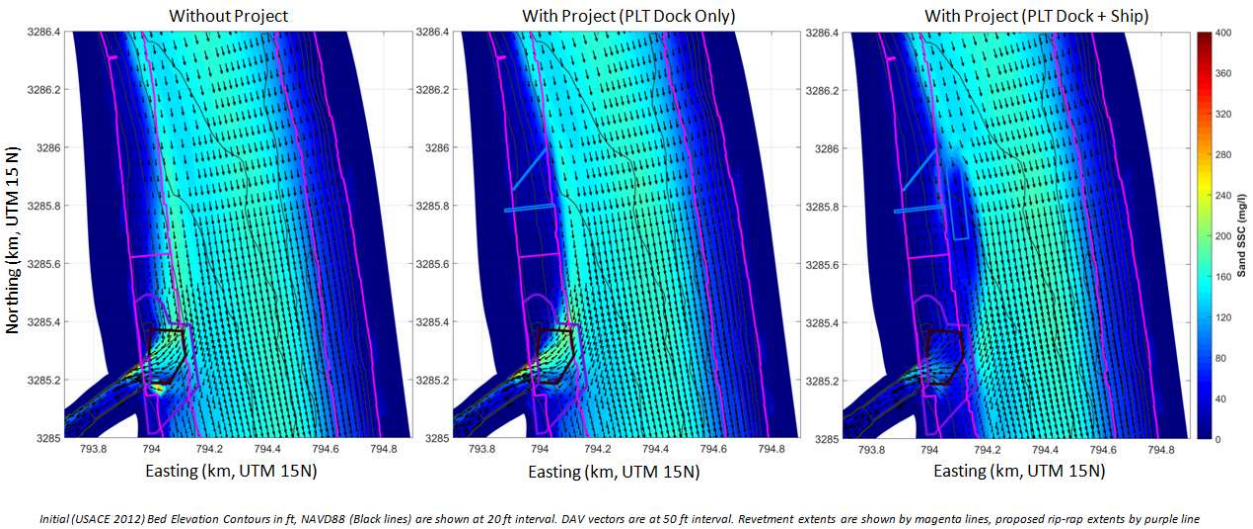

Figure 5.21. No Morphology Change: Near-bed Suspended Sand Concentration (SSC) at 800,000 cfs MR flow.

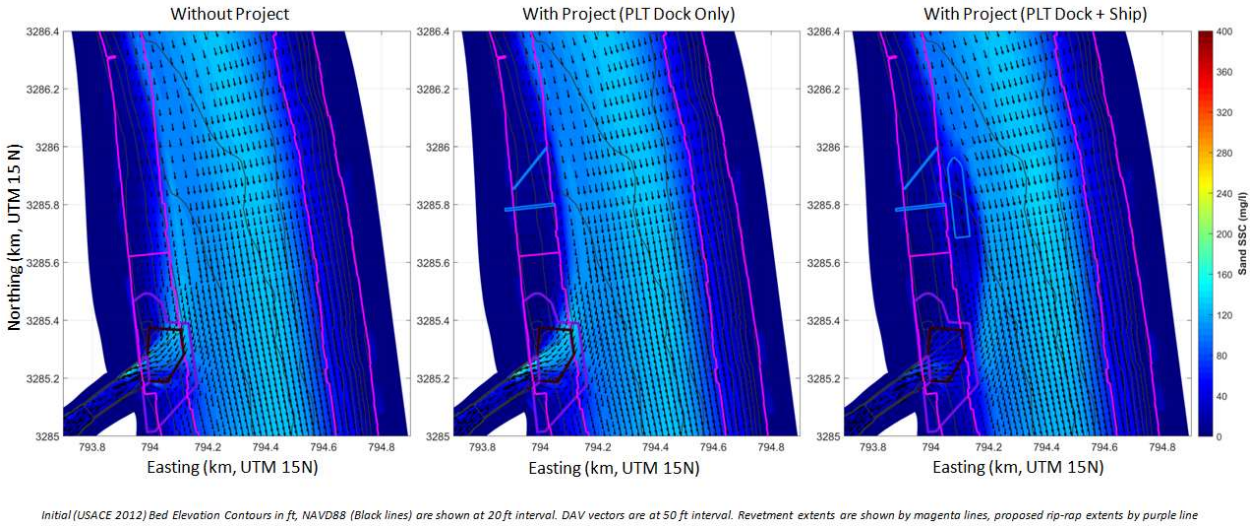

Figure 5.22. No Morphology Change: Near-bed Suspended Sand Concentration (SSC) at 600,000 cfs MR flow.

Figure 5.23 shows the variation of the diverted total sediment (Sand+Fines) load and corresponding CSWR (over 100,000 cfs discharge bins) with MR discharge. The reduction, under With-Project condition, as percentage of the Without-Project condition is also shown. Since the fines have a comparatively lesser reduction than the sand and the because fines load area about 2-3 times higher than the sand load in the river, the net reduction effect in the total sediment is less compared to that of sand alone. While total sediment loads and changes in them,

are reported, it should be noted that, the total fines captured, is reduced in approximately similar proportion as the reduction in diverted discharge due to the effects of the PLT Dock and/or the ship. This is because, the fines are well-mixed in the water column. Therefore, the critical sediment impact efficiency parameter is the reduction in sand load in addition to the hydrodynamic impact efficiency parameter of the reduction in diverted discharge. However, the reduction of the total sediment due to the presence of the PLT ship at MR flows greater than 900,000 cfs is higher (15-20%) compared to that at flows lesser than 900,000 cfs flows (5-10%).

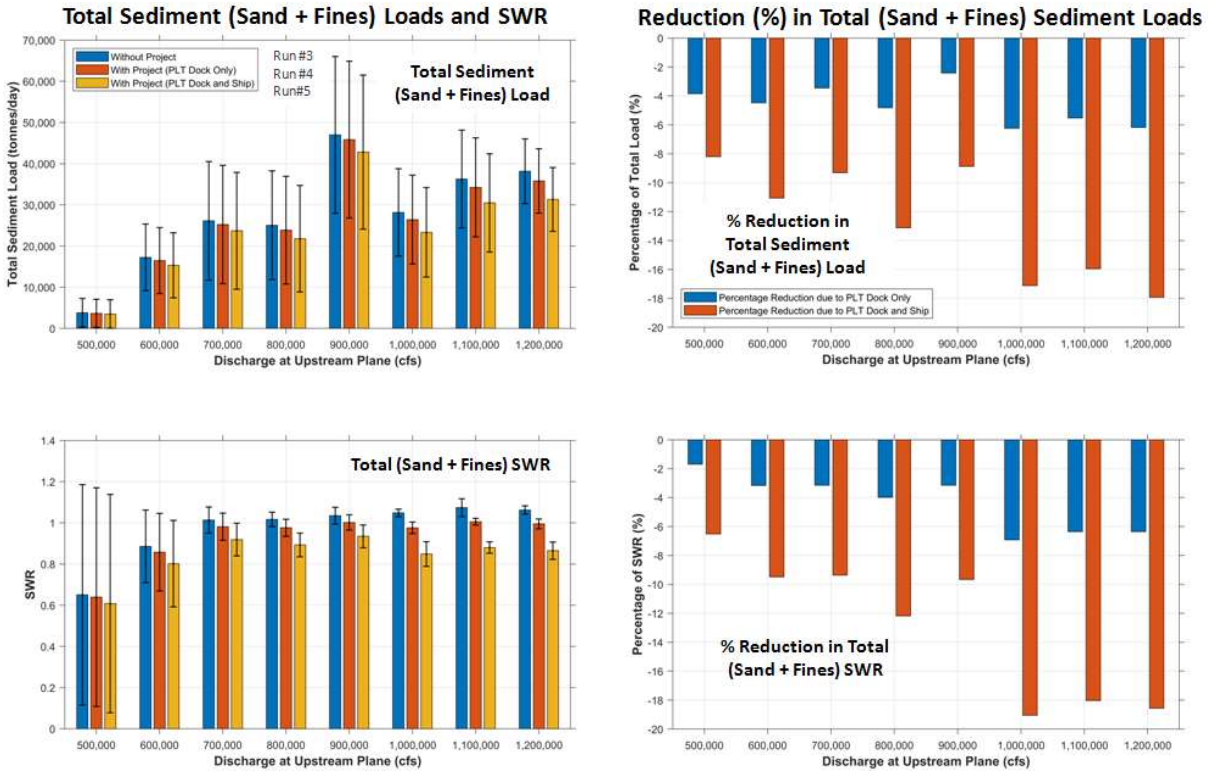

Figure 5.23. No Morphology Change: Variation of Total Sediment (Sand+Fines) and Total SWR (left panel) and percent reduction from Without-Project scenario of Total Sediment and Total SWR (right panel) with MR flow. Model run was using the 2008 hydrograph year for the entire operational period.

Figures 5.24 and 5.25 present model results from the with-morphology-change (but with non-erodible initial bed) runs (Runs 6, 7 and 8) and quantify effects of the PLT Dock and PLT Dock+Ship separately on the net reduction, similar to Figures 5.18 and 5.23. The main difference from the no-morphology-change runs is that these model runs take into consideration the temporal change in bed level and the effect of the bed material load supply to the diverted

sediment load, which can be locally deposited and eroded into the diversion, depending on the flow. Thus, the diverted loads are slightly higher at the higher flows (when sediment deposited at lower flows is available for transport) and lower at the lower flows (where the sediment being deposited in the river reduces the diverted load). Nevertheless, the reduction in the range of variation in the presence and absence of the ship is seen to be higher (30-45%) at MR flows exceeding 900,000 cfs than at lesser flows (15-20% reduction).

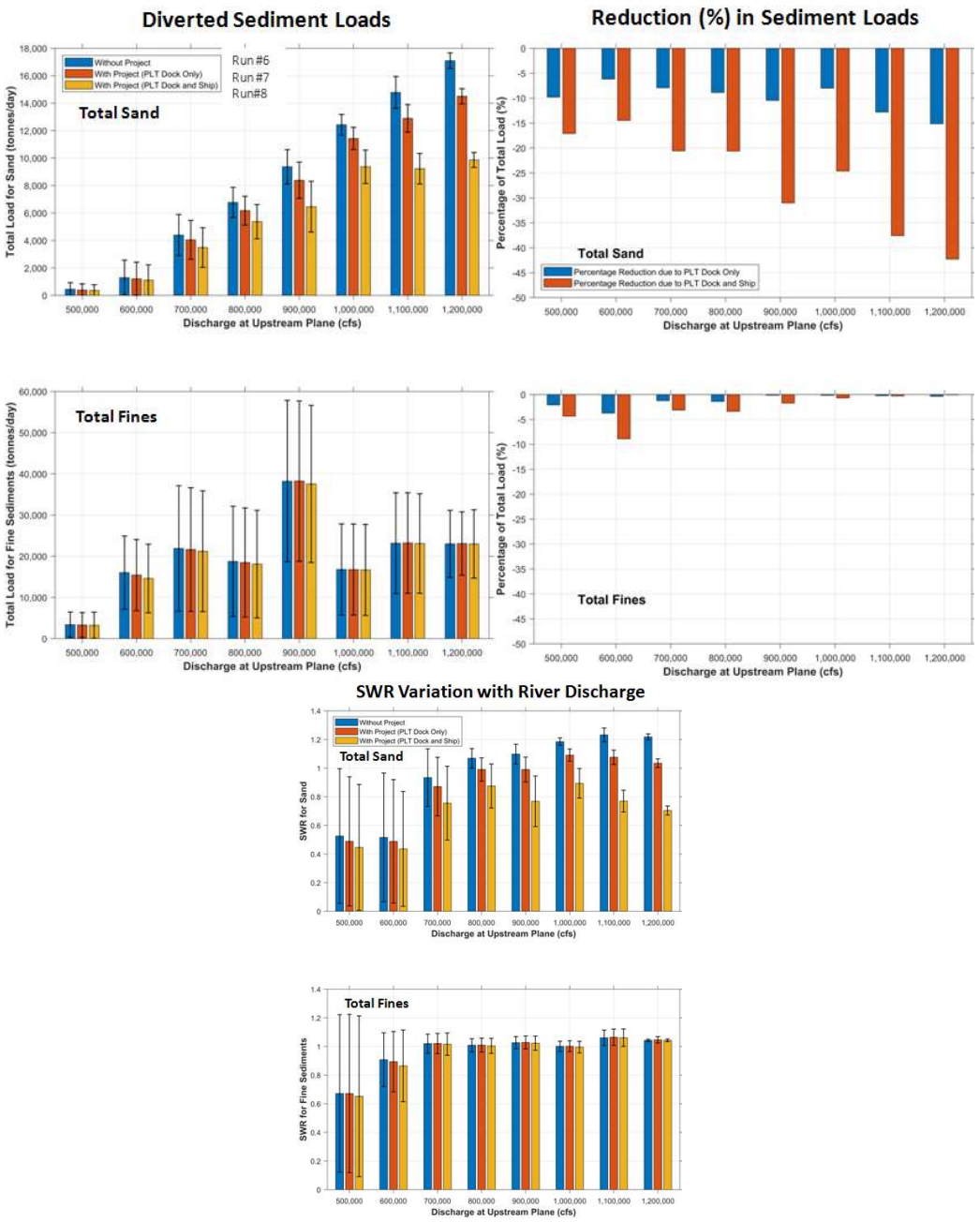

Figure 5.24. With morphology-change, non-erodible initial bed: variation of Total Sand and Fines loads (upper left panel) and percent reduction from-Without-Project scenario with MR flow. Bottom panel shows the variation in SWR of Total Sand and Fines. Model run was using the 2008 hydrograph year for the entire operational period.

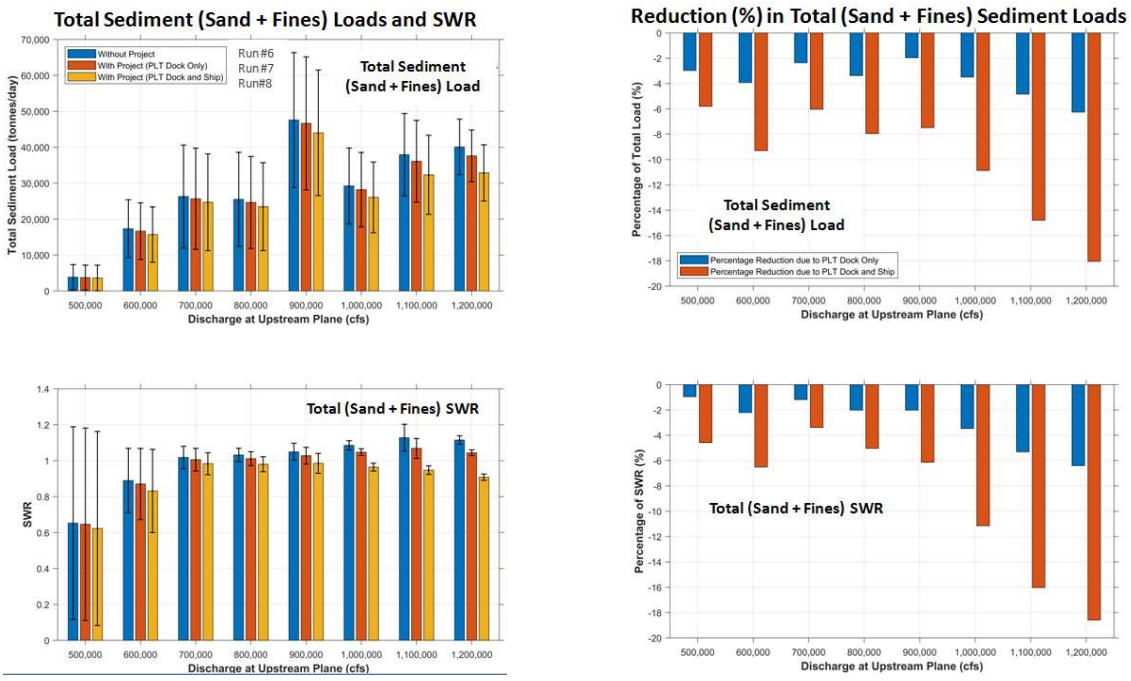

Figure 5.25. With-morphology-change, non-erodible initial bed: variation of Total Sediment (Sand+Fines) and Total SWR (left panel) and percent reduction from Without-Project scenario of Total Sediment and Total SWR (right panel) with MR flow. Model run was using the 2008 hydrograph year for the entire operational period.

Tables 5.3 and 5.4 show the annual estimations of diverted sediment loads, water volume, CSWR along with reduction percentages under with-structure scenarios with respect to the without-structure scenario. The upper panels in Table 5.3 and 5.4 respectively show the total annual water volume and sediment load diverted as well as that passing the river section, for the No-Morphology-Change (Runs 3,4 and 5) and With-Morphology-Change (Runs 6, 7, and 8) scenarios. The lower panel in the two tables shows the percent reduction under the With- Project scenarios. It is seen that the percent reduction in the sand load varies between ~11-15 % due to the PLT Dock only and between ~30-45% due to the combined effect of the PLT Dock and the Ship. Estimated reduction in fines load is less than 1% due to the PLT Dock only and between 1-5% due to the combined effect of the dock and the ship. The reduction in total sediment load is between 4-5% due to the PLT Dock only 11-14% due to the combined effect of the PLT Dock and the ship. The lower and upper ranges of the reduction are based on whether the model is run with or without morphology change and provide modeling results variability expected from the differing assumptions.

Table 5.3. No Morphology Change (Runs # 3, 4 and 5). Upper Panel: Sediment Loads and CSWR. Lower Panel: Percent Reduction for each With-Structure scenario compared to the Without-Structure scenario.

Case	Total Sand Load Diverted (MMT) (A)	Total Fines Load Diverted (MMT) (B)	Total Sediment Load Diverted (MMT) (C)	Total Sand Load in River (MMT) (D)	Total Fines Load in River (MMT) (E)	Total Sediment Load in River (MMT) (F)	Total Water Volume Diverted (TCF) (G)	Total Water Volume in River (TCF) (H)	Sand CSWR (-) (A/D)÷(G/H)	Fines CSWR (-) (B/E)÷(G/H)	Total CSWR (-) (C/F)÷(G/H)
Run#3 Without Project	1.48	3.69	5.17	19.29	47.69	66.98	1.01	13.35	1.01	1.02	1.02
Run#4 With Project (PLT Dock Only)	1.26	3.66	4.92	19.28	47.67	66.95	1.00	13.35	0.87	1.02	0.98
Run#5 With Project (PLT Dock + Ship)	0.85	3.60	4.45	19.27	47.62	66.89	0.99	13.35	0.60	1.02	0.90

MMT = Million Metric Ton (or Million Tonnes); TCF = Trillion Cubic Feet. Values are rounded to the second decimal place.

Percent Reduction with Respect to Without Project Case:

Case	Reduction in Total Sand Load Diverted (%)	Reduction in Total Fines Load Diverted (%)	Reduction in Total Sediment Load Diverted (%)	Reduction in Total Sand Load in River (%)	Reduction in Total Fines Load in River (%)	Reduction in Total Sediment Load in River (%)	Reduction in Total Water Volume Diverted (%)	Reduction in Total Water Volume in River (%)	Reduction in Sand CSWR (%)	Reduction in Fines CSWR (%)	Reduction in Total CSWR (%)
Without Project	N/A	N/A	N/A	N/A	N/A	N/A	N/A	N/A	N/A	N/A	N/A
With Project (PLT Dock Only)	14.9	0.8	4.8	0.0	0.0	0.0	0.0	0.0	13.9	0.0	3.9
With Project (PLT Dock + Ship)	42.6	2.4	13.9	0.1	0.1	0.1	0.0	0.0	40.6	0.0	11.7

Percent Values are rounded to the first decimal place.

Table 5.4. With Morphology Change (Runs # 6, 7 and 8). Upper Panel: Sediment Loads and CSWR. Lower Panel: Percent Reduction for each With-Structure scenario compared to the Without-Structure scenario.

Case	Total Sand Load Diverted (MMT) (A)	Total Fines Load Diverted (MMT) (B)	Total Sediment Load Diverted (MMT) (C)	Total Sand Load in River (MMT) (D)	Total Fines Load in River (MMT) (E)	Total Sediment Load in River (MMT) (F)	Total Water Volume Diverted (TCF) (G)	Total Water Volume in River (TCF) (H)	Sand CSWR (-) (A/D)÷(G/H)	Fines CSWR (-) (B/E)÷(G/H)	Total CSWR (-) (C/F)÷(G/H)
Run#6 Without Project	1.62	3.69	5.31	19.60	47.69	67.29	1.01	13.35	1.09	1.02	1.04
Run#7 With Project (PLT Dock Only)	1.44	3.66	5.10	19.58	47.67	67.25	1.00	13.35	0.98	1.02	1.01
Run#8 With Project (PLT Dock + Ship)	1.10	3.61	4.70	19.55	47.62	67.17	0.99	13.35	0.76	1.02	0.94

MMT = Million Metric Ton (or Million Tonnes); TCF = Trillion Cubic Feet. Values are rounded to the second decimal place.

Percent Reduction with Respect to Without Project Case:

Case	Reduction in Total Sand Load Diverted (%)	Reduction in Total Fines Load Diverted (%)	Reduction in Total Sediment Load Diverted (%)	Reduction in Total Sand Load in River (%)	Reduction in Total Fines Load in River (%)	Reduction in Total Sediment Load in River (%)	Reduction in Total Water Volume Diverted (%)	Reduction in Total Water Volume in River (%)	Reduction in Sand CSWR (%)	Reduction in Fines CSWR (%)	Reduction in Total CSWR (%)
Without Project	N/A	N/A	N/A	N/A	N/A	N/A	N/A	N/A	N/A	N/A	N/A
With Project (PLT Dock Only)	11.1	0.8	4.0	0.0	0.0	0.1	0.0	0.0	10.1	0.0	2.9
With Project (PLT Dock + Ship)	32.1	2.2	11.5	0.1	0.1	0.2	0.0	0.0	30.3	0.0	9.6

Percent Values are rounded to the first decimal place.

5.4 Delft3D Model Results: Morphology

Figure 5.26 shows the deposition extents and depths at the end of 1 year, diversion open and under Without-Project, With-Project (PLT Dock only) and With-Project (PLT Dock + Ship) scenarios. It is seen that the zone immediately downstream of the CHS terminal shows deposition as expected based on the hydrodynamic results shown on Figure 4.5 This region tends to deposit even without the presence of the PLT project. In presence of the PLT Dock only, deposition is seen to extend along the RDB under the Dock and immediately upstream of the diversion on the USACE revetment. It is recommended that any expected deposition on the USACE revetment be included in the structural stability calculations of the revetment around the diversion. The presence of the ship tends to reduce the deposition under the dock as well as immediately downstream of the ship mainly due to the increased velocities (see Fig. 5.32 later for flow velocities) under and around the ship. However, the presence of the ship is seen to increase deposition at the MBSD intake within the river as well as downstream of the intake on the USACE revetment.

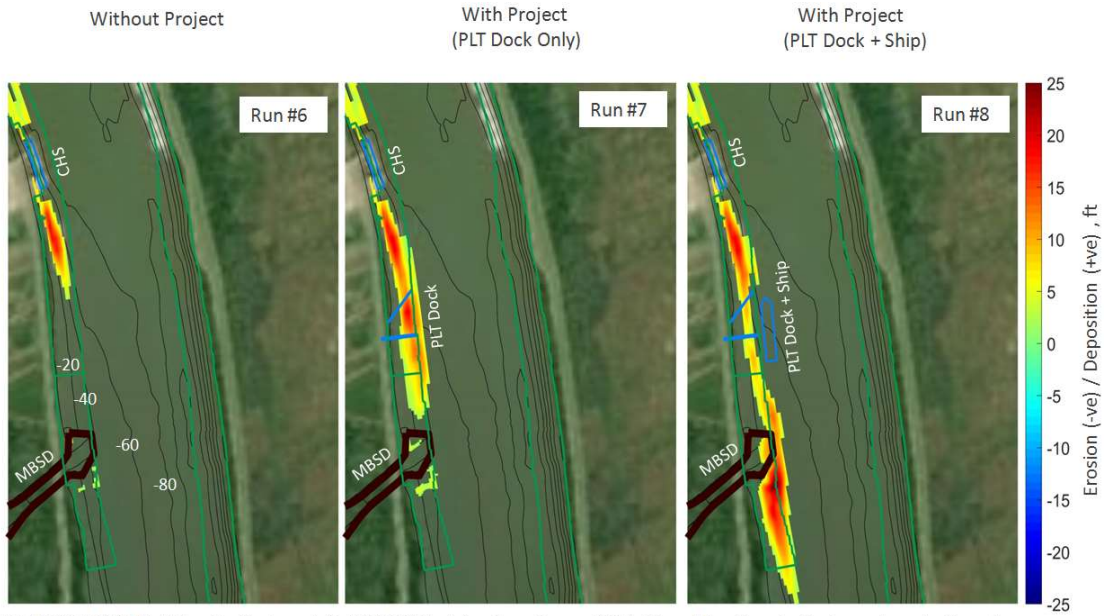

Figure 5.26. With-morphology-change, non-erodible initial bed diversion open (Runs 6, 7 and 8): deposition extents and depths at the end of 1 year of diversion operations, after immediate opening of the diversion under Without-Project, With-Project (PLT Dock only) and With-Project (PLT Dock+Ship) scenarios.

Figure 5.27 shows the difference of deposition depths at the end of 1 year between the With- and Without-Project conditions. As explained before on Figure 5.26, it appears that the existence of the PLT dock would induce deposition under the dock. In presence of the ship additional deposition is seen at the diversion intake and downstream of the diversion along the RDB.

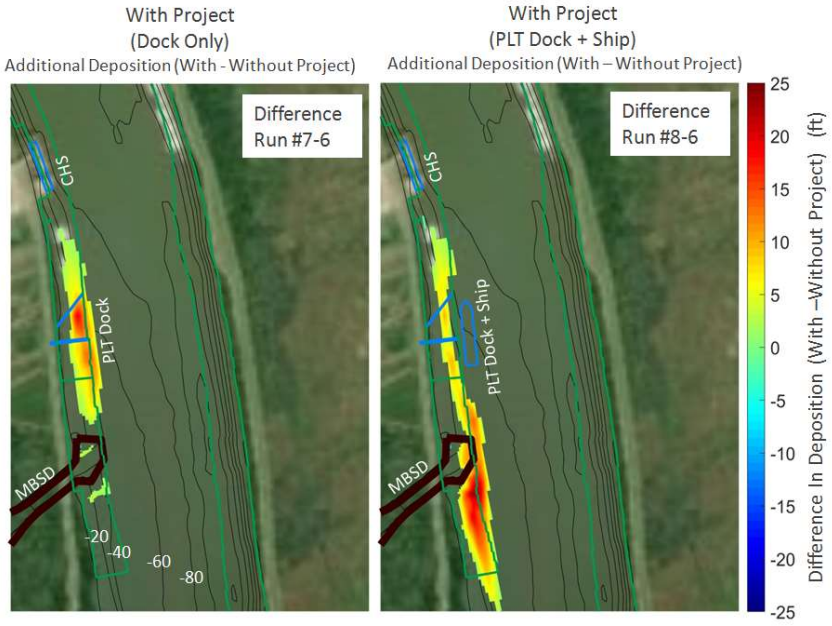

Figure 5.27. With-morphology-change, non-erodible initial bed, diversion open: difference in deposition depths (With – Without Project) at the end of 1 year of diversion operations, after immediate opening of the diversion.

Figure 5.28 shows the deposition depths and extents at the end of the same 1-year period but when the diversion is closed. Difference between the diversion open and closed deposition depths is shown in Figure 5.30. Results indicates that enhanced deposition occurs at the intake as well as between the -40 ft and -50 ft, NAVD88 contours in the river immediately in front of the intake in the presence of the ship. An interesting insight from this figure is that downstream of the diversion, the diversion open condition results in greater deposition along the shallower parts of the revetment than the diversion closed condition. This is because, when the diversion is open, the flow tends to bring the sand up on the shallower depths which otherwise remain free of deposits when the diversion is closed and the river flow is unaffected by the diversion flow.

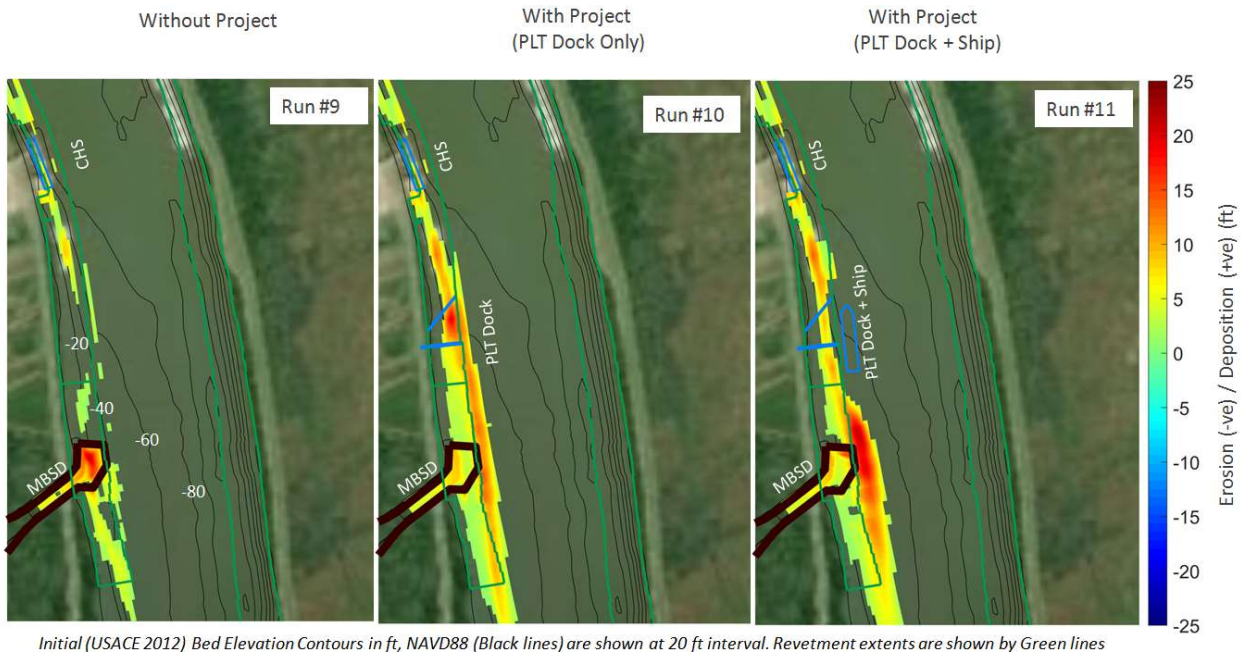

Figure 5.28. With-morphology-change, non-erodible initial bed diversion closed (Runs 9, 10 and 11): deposition extents and depths at the end of 1 year under Without-Project, With-Project (PLT Dock only) and With-Project (PLT Dock+Ship) scenarios.

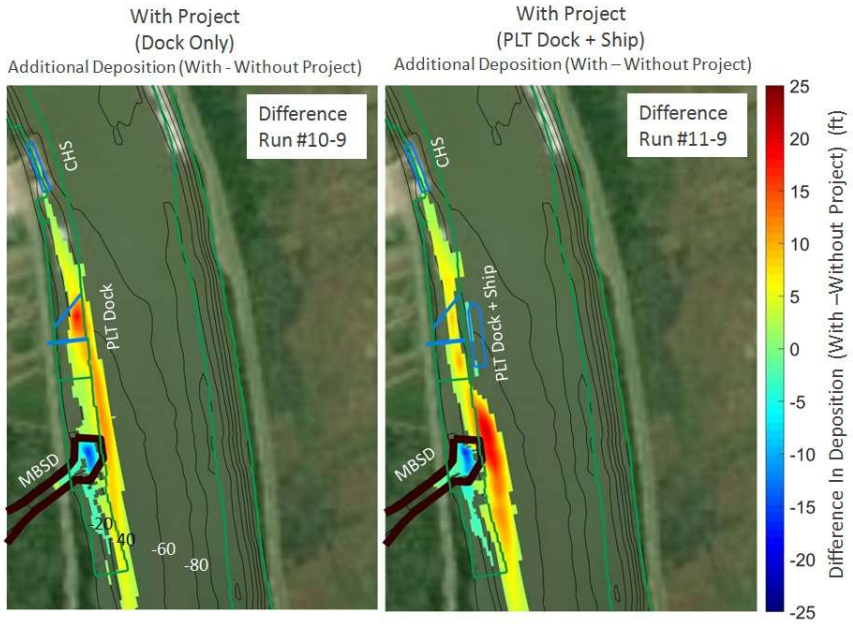

Figure 5.29. With-morphology-change, non-erodible initial bed diversion closed: Difference in deposition depths (With – Without Project) at the end of 1 year.

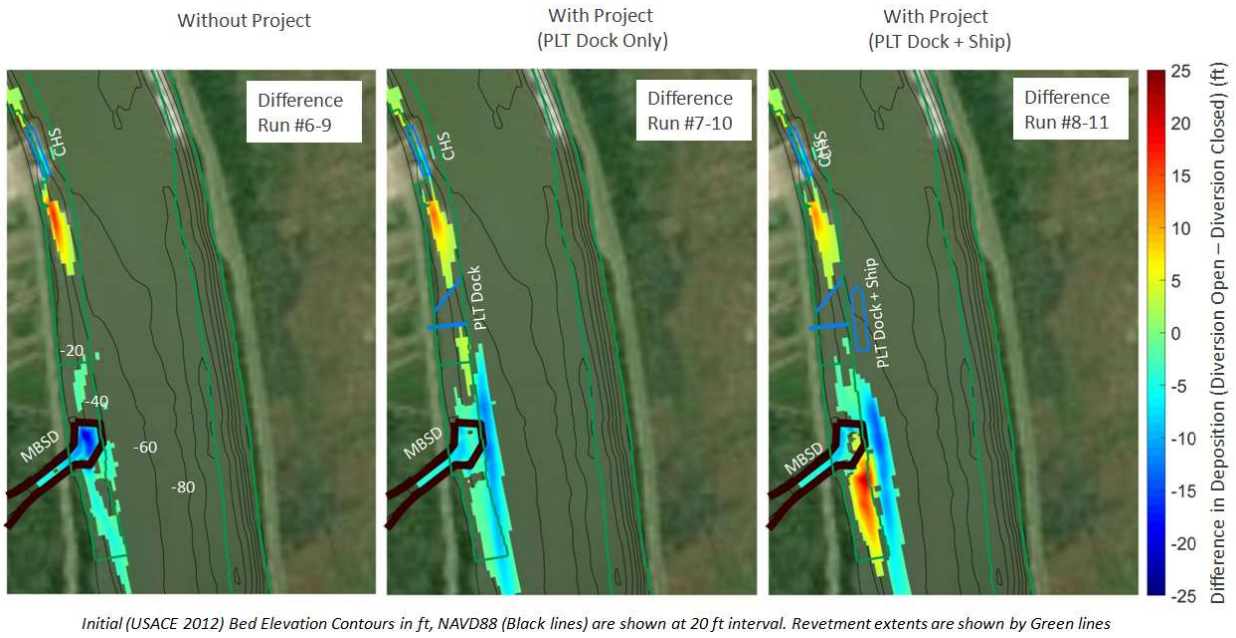

Figure 5.30. With-morphology-change, non-erodible initial bed difference in deposition depths under diversion open and closed scenarios (Open – Closed) at the end of 1 year.

Figure 5.31 shows the deposition and erosion results for the With-Project (PLT Dock + Ship) scenario at the end of 1 year. These results indicate that sandbar erosion under the ship is possible, even when a locally erodible stratigraphy is considered. It is to be noted that these results are largely qualitative because the Delft3D model is not calibrated to predict sand bar erosion rates for this study. Further investigation and verification of ship induced sand bar scour is recommended using ship scale fluid-structure interaction numerical models and/or with physical modeling. Additional stratigraphy information of sand bar using geotechnical information is also recommended to be incorporated into modeling.

Figure 5.32 shows the comparison of velocity profiles between the FLOW-3D and the Delft3D model under 'No Morphology Change' case. It is seen that except the location immediately downstream of the ship head, both models predict the velocity with good agreement indicating that the Delft3D model can be reliably taken to represent the flow under the ship. While velocities are less than 4 ft/s upstream of the ship near the bed, they increase to 4-6 ft/s under the ship due to flow constriction. It is therefore possible that the increased velocity, particularly near the bed, can thus cause erosion under the ship as predicted by the erodible bed runs.

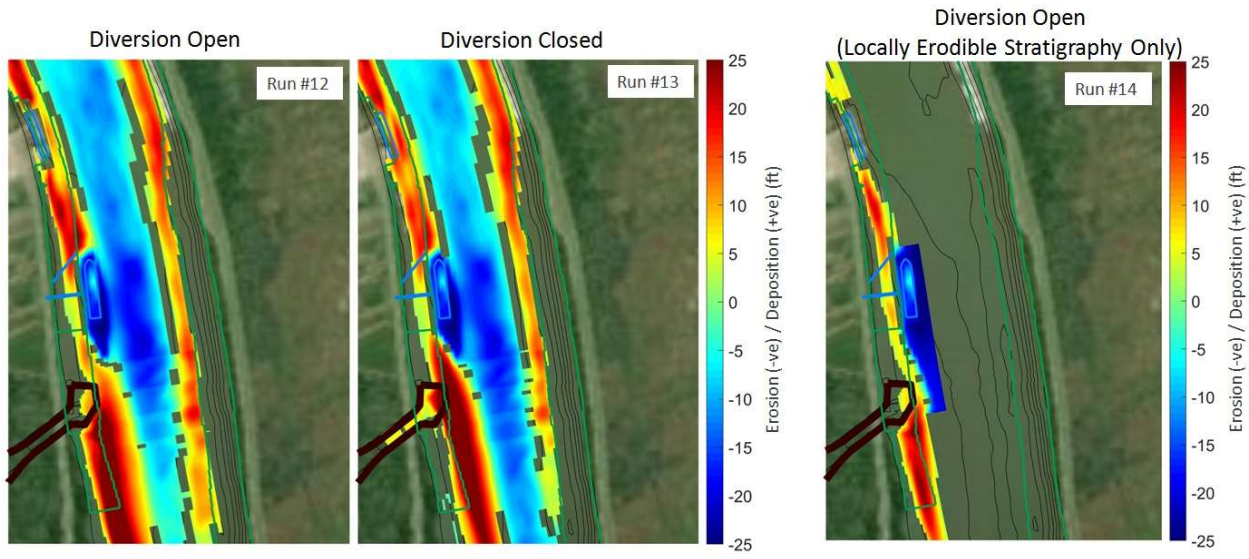

Figure 5.31. With-morphology-change, erodible initial bed (Runs 12, 13 and 14): deposition or erosion depths and extents at the end of 1 year under With-Project (PLT Dock + Ship) scenario. Left two panels are with entire river stratigraphy set as erodible with diversion open in the first panel and the diversion closed in the second. The right panel is for a model run with a locally erodible stratigraphy under the ship only.

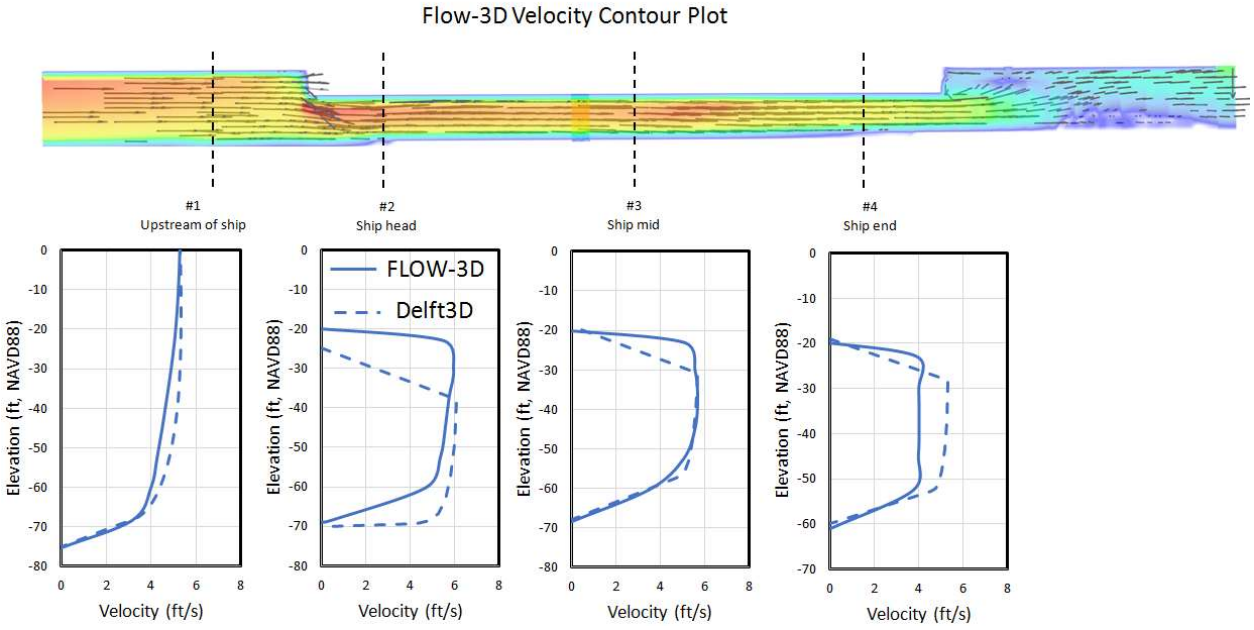

Figure 5.32. Comparison of vertical profile of velocity magnitude under the ship from FLOW-3D and Delf3D.

6.0 SUMMARY AND CONCLUSIONS

FLOW-3D and Delft3D models were developed to model the effect of the PLT Dock and Ship on the discharge capacity and the diverted sediment loads for MBSD.

Both models were calibrated/validated with observed data. In addition, the Delft3D model was calibrated with the FLOW-3D model results for hydrodynamics and diversion discharge to account for the energy losses resulting from the presence of the PLT Dock and Ship and the near-field effect of the velocity field at the intake.

The PLT Dock structure was represented as porous mesh planes following existing modeling methodology by CPRA (Meselhe et al., 2012). The porosity and drag confidents were based on values in published literature and empirical studies and depend on the structural resistance to flow for portions of the dock that are under water.

The Delft3D (3D) sediment transport model was run to evaluate effect on diverted loads, SWR as well as short term morphology change in the vicinity of the diversion and the PLT Dock. Morphology and sediment transport model results are representative of the *immediate effect in one year* of diversion opening in response to a historical (2008) hydrograph. The effects of PLT Dock and Ship on diversion sediment capture efficiency and subsequent morphological response of the river in the vicinity of the intake and along the RDB were evaluated.

The following conclusions can be drawn from this modeling study:

1. Estimated changes in *hydrodynamics* due to the presence of PLT Dock Only are as follows:
    a. ~2.4% reduction in diverted discharge at 1M cfs MR flow
    b. ~0.1-0.3 ft of Total Energy Head reduction at MBSD intake at 1M cfs MR flow
    c. Riverside intake velocities reduce from ~ 5 ft/s to ~2.5-4 ft/s at 1M cfs MR flow
2. Estimated change in *hydrodynamics* due to the presence of PLT Dock and Ship are as follows:
    a. ~4.3% reduction in diverted discharge at 1M cfs MR flow
    b. ~0.3-0.5 ft of Total Energy Head reduction at MBSD intake at 1M cfs MR flow

c. Riverside intake velocities reduce from ~ 5 ft/s to ~1.5-2.3 ft/s at 1M cfs MR flow

3. Estimated reductions of sediment load due the presence of PLT Dock only are as follows:

   a. ~11-15 % for diverted sand load

   b. ~0-1 % for diverted fines load

   c. ~4-5 % for diverted total load

4. Estimated reduction of sediment load due the combined presence of PLT Dock and Ship (moored during the entire operational period) are as follows:

   a. ~30-45 % for diverted sand load

   b. ~4-5 % for diverted fines load

   c. ~11-14 % for diverted total load

5. The reduction in sediment loads estimated above in # 4 for PLT Dock and Ship scenario may be lower if intermittent ship operations are included in the analysis. However, the reduction, including intermittent ship operations, will still be greater than the reduction due to the PLT Dock alone mentioned in # 3.

6. Uncertainty in the reported reduction percentages include but are not limited to the following factors which are not considered in this study:

   - Nature of the MR Hydrograph
   - Long-term morphological impacts of the PLT Dock and/or ship
   - Frequency and timing of ship operations within the hydrograph period
   - Variation in ship draft
   - Local fluid-structure scale transient effects on the sediment transport and sand bar scour
   - Ship motion induced sediment transport and morphology change
   - Sensitivity of model to drag coefficients used to parameterize the structure losses

7. Deposition was noted under the PLT Dock, along the RDB and on the USACE revetment downstream of the diversion when the ship was present. Additional long-term numerical modeling and/or physical modeling is suggested to verify the evolution of this zone and its impact on sediment capture and hydrodynamics.

8. Increased deposition is noted at the diversion intake under diversion closed scenario due to the presence of the PLT Dock.

9. Presence of the stationary ship indicates some erosion of the native sand-bar due to the increased near-bed velocities under the ship. This model does not take into account the effect of ship movements on morphology. Additional numerical modeling at the fluid-structure interaction scale of the ship and/or physical modeling is recommended to verify this.

10. Dredging to maintain required ship draft at the PLT location can affect the stability of the sand-bar, which is the main platform over which sand travels towards the diversion intake and enables the intake to access the near bed high sand concentration zone.

11. The Delft3D model does not model head-cut propagation, bank collapse, scour under the revetment or rip-rap. Morphology results should be used with caution when using the absolute deposition/erosion depths for design.

7.0 REFERENCES

Achenbach, E. 1971. *Influence of surface roughness on the cross-flow around a circular cylinder*, Journal of Fluid Mechanics, 46(2), 321-335.

Allison, M.A. 2011. *Water and Sediment Surveys of the Mississippi River Channel Conducted at Myrtle Grove and Magnolia in Support of Numerical Modeling (October 2008 to May 2011*. Technical Report to Louisiana Coastal Protection and Restoration Authority from the Water Institute of the Gulf.

Allison, M.A., Demas, C., Ebersole, B., Kleiss, B., Little, C., Meselhe, E., Powell, N., Pratt, T., Vosburg, B. 2012. *A Water and Sediment Budget for the Lower Mississippi-Atchafalaya River in Flood Years 2008-2010: Implications for Sediment Discharge to the Oceans and Coastal Restoration in Louisiana*. Journal of Hydrology 432-433 pp84-97.

Allison, M.A., Brendan, T. Y., Meselhe, E.A., Marsh, J.K., Kolker, A.S., Ameen, A.D. 2017. *Observational and numerical particle tracking to examine sediment dynamics in a Mississippi River delta diversion*. Est. Coast. Shelf Sc., 194, pp97-108

Allison, M.A., Di Leonardo D.R., Eckland, A.C., Ramatchandirane C., Weathers H.D. 2018. *Mid-Barataria Technical Team Field Data Support*. The Water Institute of the Gulf. Prepared for and funded by the Coastal Protection and Restoration Authority. Baton Rouge, LA.

Blevins, R.D. 1984. Applied Fluid Dynamics Handbook. Van Nostrand Reinhold Co., New York, N.Y.

Chamsri, K. and Schreyer, L. 2015. *Permeability of Fluid Flow Through a Periodic Array of Cylinders*. Applied Mathematical Modeling, 39(1), 244-254.

Deltares. 2018. *Delft3D FLOW, User Manual: Simulation of multi-dimensional hydrodynamic flows and transport phenomena, including sediments*. Delft, The Netherlands.

Esposito, C., Liang, M., Meselhe, E. 2017. *TO5 Outfall Management Mid-Barataria and Mid-Breton Diversions*. Technical Report to Louisiana Coastal Protection and Restoration Authority from the Water Institute of the Gulf.

Flow Science. 2018. *Version 12.0 User's Manual FLOW-3D [Computer software]*. Santa Fe, NM: Flow Science, Inc.

Gaweesh, A., Meselhe, E. 2016. *Evaluation of Sediment Diversion Design Attributes and Their Impact on the Capture Efficiency*. Journal of Hydraulic Engineering 142 Issue 5

HDR. 2014. *Mid-Barataria Sediment Diversion Alternative 1, Base Design Report 30% Basis of Design.* Technical Report to the Louisiana Coastal Protection and Restoration Authority.

Liang, M., Esposito, C., Meselhe E. 2017. *Technical Memorandum Mid-Barataria Invert Elevation and Outfall Channel Configuration.*

McCorquodale, A., Amini, S., Teran, G., Gurung, T., Kenny, S., Gaweesh, A., Pereira, J. and Meselhe, E. 2016. *Development of a Regional 3-D Model for the Lower Mississippi River*. Joint UNO – Louisiana Coastal Protection and Restoration Authority. Technical Report from the Water Institute of the Gulf.

Meselhe, E., Richardson, J., Roberts H., Lagumbay, R.2012. *RAM Terminal CFD Modeling Technical Memorandum*. Louisiana Coastal Protection and Restoration Authority. Technical Report from the Water Institute of the Gulf.

Meselhe, E., Georgiou, I., Allison, M. and McCorquodale, J. 2012a. *Numerical Modeling of Hydrodynamics and Sediment Transport in Lower Mississippi at a Proposed Delta Building Diversion. Journal of Hydrology*, 472-473, 340-354.

Meselhe, E.A., Baustian, M.M., Allison, M.A. 2015. *Basin-wide model development for the Louisiana Coastal Area Mississippi River hydrodynamic and delta management study. The Water Institute of the Gulf*. Prepared for and funded by the Coastal Protection and Restoration Authority. Baton Rouge, Louisiana.

Meselhe, E., Sadid, F., Messina, F., Jung, H. 2017. *Technical Memorandum TO46: Basin-Wide Delft Evaluation of Diversion Operations (Production Runs 11-15)*. Louisiana Coastal Protection and Restoration Authority. Technical Report from the Water Institute of the Gulf.

Partheniades, E. 1965. *Erosion and Deposition of Cohesive Soils*. Journal of the Hydraulics Division, ASCE 91 (HY 1): 105–139.

Rijn, L. C. van. 1993. *Principles of Sediment Transport in Rivers, Estuaries and Coastal Seas.* Aqua Publications, The Netherlands.